
DYNAMIC TENSOR REMATERIALIZATION

A PREPRINT

Marisa Kirisame^{*†}
jerry96@cs.washington.edu

Steven Lyubomirsky^{*†}
sslyu@cs.washington.edu

Altan Haan^{*†}
altanh@cs.washington.edu

Jennifer Brennan^{*}
jrb@cs.washington.edu

Mike He^{*}
dh63@cs.washington.edu

Jared Roesch^{*‡}
jroesch@cs.washington.edu

Tianqi Chen^{*‡}
tqchen@cs.washington.edu

Zachary Tatlock^{*}
ztatlock@cs.washington.edu

June 19, 2022

ABSTRACT

Checkpointing enables training larger models by freeing intermediate activations and recomputing them on demand. Previous checkpointing techniques are difficult to generalize to dynamic models because they statically plan recomputations offline. We present Dynamic Tensor Rematerialization (DTR), a greedy online algorithm for heuristically checkpointing *arbitrary* models. DTR is extensible and general: it is parameterized by an eviction policy and only collects lightweight metadata on tensors and operators. Though DTR has no advance knowledge of the model or training task, we prove it can train an N -layer feedforward network on an $\Omega(\sqrt{N})$ memory budget with only $\mathcal{O}(N)$ tensor operations. Moreover, we identify a general eviction heuristic and show how it allows DTR to automatically provide favorable checkpointing performance across a variety of models and memory budgets.

1 Introduction

As state-of-the-art deep learning (DL) models continue to grow [1, 2, 3], training them within the constraints of on-device memory becomes more challenging. Memory constraints prevent training models on certain devices (including specialized accelerators in distributed settings and some low-powered mobile devices) and also limit batch sizes. Checkpointing techniques can enable processing larger models and batches that otherwise do not fit in on-device memory, without modifying the model’s design. This is achieved by trading additional computation for memory savings: some activations are freed and recomputed on demand. Adapted from techniques in automatic differentiation (AD) [4, 5, 6], checkpointing in the DL context exploits the fact that intermediate activations for backpropagation dominate memory usage during training [7] but can be easily recomputed by replaying parts of the forward pass. Current DL checkpointing techniques [8, 9, 10, 11] *statically* plan which values to checkpoint offline, requiring advance knowledge of a model’s control flow. Unfortunately, this requirement excludes applications with general data-dependent control flow, including many dynamic models [12, 13, 14] and meta-learning applications [15, 16].

We present Dynamic Tensor Rematerialization (DTR), a new greedy online checkpointing algorithm for heuristically checkpointing *arbitrary* models. DTR operates like a tensor-level cache: it collects metadata on tensors and operators as a model is trained, and then uses this metadata to choose which activations to free and later recompute. Metadata is gathered dynamically, so it precisely tracks tensor sizes, operator costs, and access times; this eliminates the need for synthetic cost models or user annotations. Because DTR requires no advance knowledge of the model or training

^{*}Paul G. Allen School of Computer Science & Engineering, University of Washington, Seattle, WA

[†]Equal contribution.

[‡]OctoML, Seattle, WA

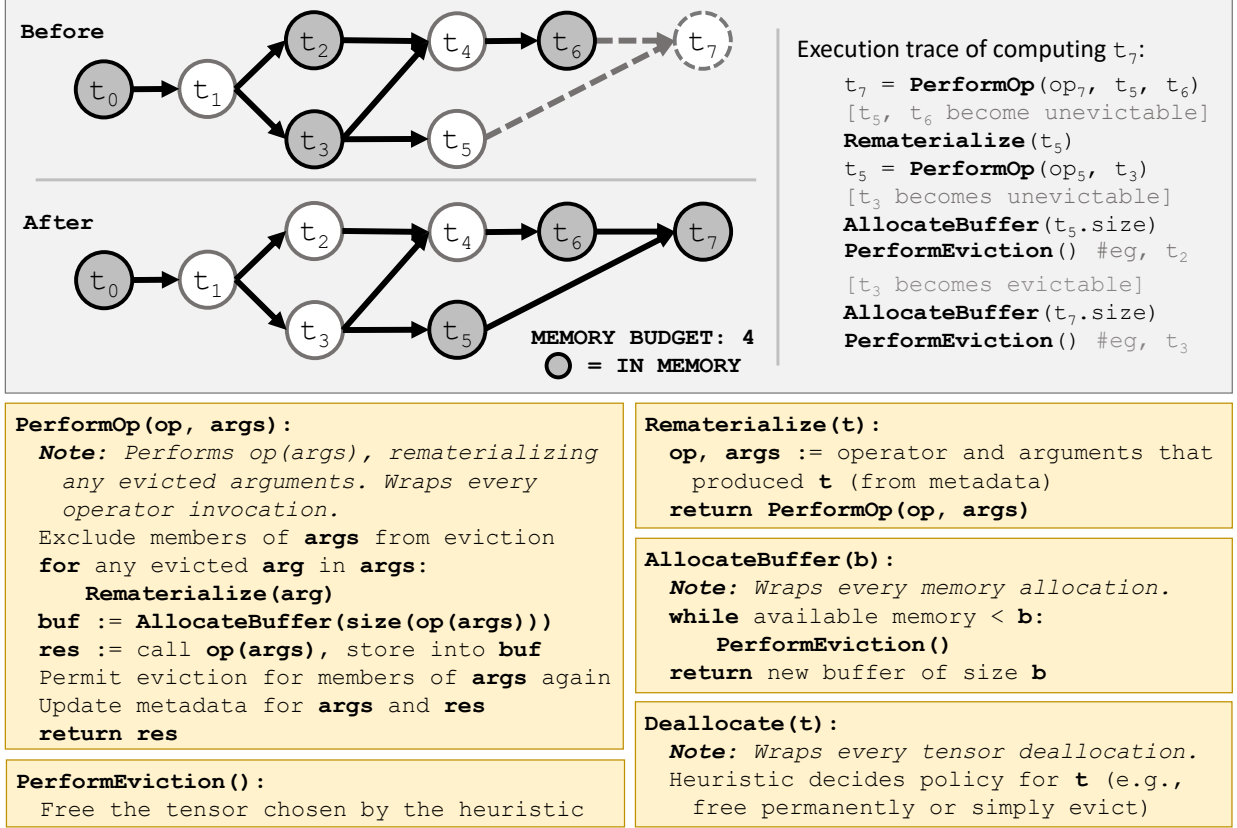


Figure 1: Pseudocode for DTR’s basic logic (independent of heuristic) and an illustration of DTR’s sequence of events in an operator call. Note that `PerformOp()` may result in further recursive calls if it needs to rematerialize arguments.

task and is parameterized by budget, it can immediately accommodate dynamic models — or, indeed, any program consisting of operations on tensors — and support varying memory requirements.

This paper describes DTR’s design (Sec. 2) and includes the following contributions:

- a proof that DTR can train an N -layer feedforward network on an $\Omega(\sqrt{N})$ memory budget with only $\mathcal{O}(N)$ tensor operations (Sec. 3), which is within a constant factor of optimal and matches the offline bound of Chen *et al.*’s [8] static checkpointing technique;
- a simulated evaluation of DTR on various static and dynamic models across a range of heuristics and memory budgets, illustrating tradeoffs involved in heuristic design and identifying h_{DTR} , a general heuristic that provides significant memory savings across diverse models (Sec. 4.1);
- a prototype implementation of DTR in the PyTorch framework [17], including practical optimizations providing well over $10\times$ speedup and further discussion of how DTR may be incorporated in DL frameworks more broadly (Sec. 4.2).

2 Dynamic Tensor Rematerialization

DTR is designed as a thin runtime layer that intercepts tensor allocations, accesses, and deallocations, eliminating the need for ahead-of-time program (e.g., DL model) analysis. Figure 1 sketches DTR’s high-level approach. When a tensor allocation occurs, DTR first checks if sufficient memory is available. If so, DTR generates a fresh tensor identifier, initializes its metadata for future recomputation, allocates the requested memory, and returns a new tensor. If not, DTR heuristically selects and *evicts* resident tensors until the requested allocation can be accommodated. Constant tensors (presumed to be external data) cannot be evicted, since there is no corresponding operation for rematerializing them. On tensor access, DTR first checks if the tensor is resident in memory. If so, DTR applies a heuristic to update tensor metadata before performing an unmodified tensor access. If the tensor has been evicted, DTR *rematerializes* [9, 10, 18] it by replaying the *parent operation* that originally produced the tensor. Crucially, rematerialization can be recursive:

if the arguments to an evicted tensor’s parent operation have also been evicted, they must also be rematerialized. Rematerialization may trigger more evictions if memory is exhausted during the potentially recursive process. On tensor deallocation, the runtime is invoked once again allowing it to update tensor metadata and eagerly perform profitable evictions. Subtle tradeoffs arise in choosing whether to *banish* (permanently free) deallocated tensors or merely treat them as evicted, as the children of banished tensors will no longer be evictable.

This abstract description of DTR assumes that tensors are only accessed by monolithic operators, tensors are either constants or produced by operators, operators produce individual tensors, and operators are pure (deterministic functions of their arguments). Under this model, a training epoch is simply a sequence of tensor operations, without any inherent requirement to recognize training-specific structure like the transition to the backward pass. DTR will evict as many tensors as necessary to avoid running out of memory. If all inputs and outputs of a single operation cannot fit into available memory, rematerialization will fail. This scenario occurs when a single operation has large arguments or during a deeply nested rematerialization. Hence, bottlenecks in the model’s design and the order in which evicted arguments are rematerialized affect the likelihood of failure.

Heuristics. DTR’s performance and overhead depend on its heuristics. As in caching, DTR’s eviction heuristic provides a *dynamic* prediction of which resident tensors are least valuable. The choice of heuristic determines what *metadata* (additional runtime facts)⁴ must be tracked for each tensor and operator, and thus the runtime overhead of DTR. Heuristics for checkpointing may consider whether a value is likely to be required for further rematerializations (making long recursive rematerializations less likely), how costly a rematerialization would be (avoiding replaying expensive computations), or how much memory an eviction would save (prioritizing evicting large tensors). For example, a heuristic like “evict the largest, cheapest, least-recently used tensor” requires DTR to track tensor sizes, costs, and access times as metadata.

We investigated several eviction heuristics, some inspired by traditional caching strategies and others devised specifically for checkpointing. These heuristics illustrate different tradeoffs with respect to metadata complexity, help validate intuitions about DTR’s behavior, and demonstrate DTR’s extensibility. Our lightweight reference heuristics include: *Random*, which evicts a random tensor; *LRU*, which evicts the least-recently accessed tensor; and *Largest*, which evicts the largest tensor, similar to *GreedyRemat* [10].

We also propose a new family of rematerialization-specific heuristics that rely on tensors’ *evicted neighborhoods*. For a resident tensor t , let $e(t)$ be the evicted, unbanished tensors t ’s parent operation depends on or whose parent operation depends on t . Let t ’s evicted neighborhood $e^*(t)$ be the set of tensors that either would need to be rematerialized to recompute t or would need t to be resident to be recomputed. For example, suppose DTR is checkpointing the network shown in Figure 1, where the resident tensors are $\{t_0, t_2, t_3, t_6\}$. Then, before node t_7 is computed, we have $e^*(t_2) = \{t_1, t_4\}$ and $e^*(t_3) = \{t_1, t_4, t_5\}$. A precise definition of $e^*(t)$ is given in Sec. C.2.

Our rematerialization-specific heuristics balance *staleness* (time since last access), memory, and the estimated rematerialization cost (approximations of $e^*(t)$) to select tensors to evict. We define these heuristics by parameterizing over measures of staleness s , memory m , and compute cost c : $h_{DTR}(s, m, c)(t) = c(t)/[m(t) \cdot s(t)]$ such that a tensor t minimizing $h_{DTR}(s, m, c)(t)$ will be evicted when memory becomes full. For a given tensor t , its staleness can be estimated by tracking the time it was last used in a computation and its rematerialization cost can be estimated by summing computation times over the evicted neighborhood $e^*(t)$. We define an equivalence class data structure to approximate the rematerialization costs without dynamically tracking evicted neighborhoods (which loses information but is cheaper to maintain dynamically). Appendix C includes a description of this data structure, as well as other metadata that heuristics can track.

Deallocation policies also present different considerations, since tensors marked as deallocated by the original program can still potentially be used for rematerializations. For instance, banishing deallocated tensors can save memory immediately (and is the only way to free constants, which cannot be evicted) but can prevent possible evictions (children of banished tensors cannot be rematerialized), while not banishing them increases management overhead and can keep constants in memory longer. In our h_{DTR} heuristics, we implemented an *eager eviction* mechanism, which evicts tensors as soon as all external references to it are freed (*i.e.*, it can be garbage collected). This allows DTR to follow the garbage collection pattern of the underlying framework, preempting desirable evictions that would occur later on, which further reduces runtime overhead. We compare the above heuristics and their tradeoffs in our evaluation (Sec. 4.1) and discuss an even broader class of heuristics in Appendix C.

⁴ In the DL domain, DTR’s metadata overhead is low relative to the cost of typical tensor operations.

3 Formal Bounds

Following [8], we prove a bound on DTR’s checkpointing overhead (for a particular eviction heuristic) on a linear feedforward network of N nodes. Even without the ability to inspect the model, DTR requires only $\mathcal{O}(N)$ tensor operations under a \sqrt{N} memory budget, the same bound (up to constant factors) as existing static checkpointing techniques [8] and the optimal $\Theta(N)$ required by a memory-unconstrained algorithm. We also establish that DTR’s dynamic approach cannot always match static checkpointing: given N tensor operations and a memory budget of B , under any deterministic heuristic an adversary can always construct a network where DTR will perform a factor of $\Omega(N/B)$ more tensor operations than a (potentially expensive [9]) optimal static checkpointing algorithm.

Linear Feedforward Overhead. We assume that tensor computations dominate runtime and, as in prior work [5, 8, 19, 20], that each tensor is of unit space and time cost. For the proof below, we use the heuristic h_{e^*} which chooses to evict a resident tensor t with minimal $|e^*(t)|$.

Theorem 3.1. *Given an N node linear feedforward network and memory budget $B = \Omega(\sqrt{N})$, DTR with heuristic h_{e^*} can execute one forward and one backward pass in $\mathcal{O}(N)$ operations.*

Proof Sketch. During the forward pass, DTR performs exactly N tensor operations: since each node of the linear feedforward network only depends on the previous node, no rematerialization is necessary. Our heuristic h_{e^*} , which evicts tensors with the smallest evicted neighborhoods, ensures that the B tensors resident at the conclusion of the forward pass are evenly spaced throughout the network. In turn, these evenly spaced checkpoints ensure DTR never has to successively rematerialize too many tensors. As the backward pass proceeds and checkpoint tensors can be freed, the overhead to compute all gradients between the checkpoints k and $k + 1$ shrinks as $\log(k)/k^2$, which converges to a constant. The full proof of Theorem 3.1 is provided in Appendix A.

Adversarial Overhead. Using a simple heuristic, DTR can match the performance of static checkpointing on linear feedforward networks, despite lacking advance knowledge of the architecture. However, DTR cannot always match the performance of optimal static checkpointing on an arbitrary network because DTR cannot access or reorder the network.

Theorem 3.2. *For any deterministic heuristic h , there exists an N -node network on which DTR with budget $B \leq N$ requiring $\Omega(N/B)$ times more tensor computations than optimal static checkpointing.*

Proof Sketch. Generate an adversarial network G of B linear feedforward networks joined by a common parent tensor. Using h , schedule G ’s operations such that, at each step of DTR, the next operation is taken from the end of an entirely evicted path through G , forcing DTR to rematerialize the entire path. DTR can thus be forced to perform at least $\Omega(N^2/B)$ operations. In contrast, an optimal static algorithm can reorder G to compute each feedforward network sequentially, requiring only N computations. The full proof of Theorem 3.2 is provided in Appendix B.

Theorems 3.1 and 3.2 illustrate how DTR’s performance, from optimal to poor, depends on interactions between heuristics and models. To explore DTR design tradeoffs, the following sections consider various heuristics and empirically evaluate DTR on a range of popular of DL models.

4 Evaluation

4.1 Simulated Evaluation

To characterize DTR’s performance on a broader class of models under various heuristics, we simulated DTR on traces gathered from PyTorch executions for several popular kinds of DL models. We describe how an existing DL framework can be extended to support simulating dynamic checkpointing techniques and detail how DTR performs under various heuristics in simulation. We find that a certain class of heuristics performs well across a range of model architectures, achieving competitive simulated performance. Furthermore, we investigate cases where DTR misses opportunities to save more memory and propose potential solutions to enable further savings. In addition to enabling rapid prototyping and evaluation of heuristics, the simulator⁵ is also a useful testing ground for revisions to the abstract description in Figure 1 to account for implementation-specific details like mutation, serving as a stepping stone to integrating DTR in full-fledged DL frameworks (Sec. 4.2).

Gathering and Simulating Execution Logs. To estimate DTR’s overhead while checkpointing a model M under heuristic h , we train M on a device with sufficient memory and log each tensor operation, allocation, and deallocation along with tensor sizes and any other dynamic information h requires (e.g., computation costs). Given such a log ℓ and a memory budget B , our simulator replays events from ℓ while tracking the total size of resident memory and updating heuristic metadata. If an allocation would cause resident memory to exceed B or an operation depends on an evicted

⁵Publicly available at <https://github.com/uwsaml/dtr-prototype>.

tensor, our simulator calculates what evictions and rematerializations DTR would perform according to h . Once all events from ℓ have been processed, the simulator reports the total number of rematerializations as well as their costs and sizes to estimate DTR’s overhead.

To gather execution logs from popular DL models, we instrumented PyTorch as its define-by-run strategy [17] is well-suited to dynamic models, though our overall strategy is framework-agnostic. Our logs record all tensor operations (including sizes, GPU compute times, and parent tensor), allocations, and deallocations. In order to faithfully capture the semantics of PyTorch DL models, simulator and logs support low-level implementation details [21] such as aliasing, multi-output tensor operations, and tensor mutation. To support aliasing, we distinguish between tensors and their underlying buffers, modeling tensors as *views* of buffers. We observed that most buffers have a small number of views (typically one), so we refer simply to “tensors” below, for simplicity. Tensors produced by multi-output operations are rematerialized together but evicted separately. While DTR assumes operators are pure, impure operators like batchnorm or dropout are made pure by treating state (*e.g.*, the PRNG seed) as an input to the operator. Similarly, operators that mutate tensors are made pure using a copy-on-write reference layer, which clones a tensor and mutates the clone. A full technical specification of the simulator is provided in Appendix C.

Experiments. We ran our simulator on logs generated from a variety of models, with results given in Figure 2. We chose three static vision models [22, 23, 24] investigated in previous work [9] and three dynamic models [25, 26, 16] that exhibit different kinds of control flow. The vision models were run on batches of 32 with 3-channel images (size 32×32 for ResNet and DenseNet, 512×512 for UNet); LSTM ran on a sequence of length 32, with 10×100 entries; TreeLSTM ran on a binary tree of depth 6, with 32×100 entries; and the Unrolled GAN ran on inputs of size 512×256 . The logs used for our simulated evaluation were produced by running each model 50 times on a single input on a machine with an NVIDIA Titan V GPU (CUDA 10.1, CuDNN 7.6.4) and a 16-core AMD Ryzen Threadripper 1950X on Ubuntu 18.04, using the final “warmed-up” log. The logged portion includes executing the forward pass, computing the loss, and performing the backward pass. Importantly, we enforced the additional condition that gradients for all trainable weights be resident at the end of the simulation, in order to model the requirements for performing a full training step.

We evaluate the DTR heuristic with the following combinations of factors: direct compute summed over the full evicted neighborhood $e^*(t)$ (DTR-Full); an approximation of DTR-Full which relaxes $e^*(t)$ using disjoint-sets (DTR-EqClass); and h_{DTR} with only the direct compute of t (DTR-Local). In all cases, staleness s was estimated using last access, and memory m using tensor size. These variants of h_{DTR} performed consistently well in a broader ablation study, detailed in Appendix D.

For all simulations, we considered a heuristic to be *thrashing* if it required at least $3\times$ the amount of computation before finishing, since we assume this to be due to long chains of unfavorable rematerializations and unviable in practice.

Discussion. For all the models in Figure 2, our simulations show significant savings at reasonable compute overheads. While we were unable to implement existing static checkpointing schemes as baselines due to the complexity of aliasing and mutation (especially in the dynamic models), we note that these results save similar amounts of memory compared to expert manual modifications to models. For example, a manually optimized DenseNet-BC model [27] achieved 56.1% memory consumption at a 25.5% slowdown, while our simulated trial using DTR-EqClass yields 20.0% memory consumption at 22.7% overhead. Although these numbers are not directly comparable since the simulation does not include the dynamic analysis overhead, they illustrate that DTR (with suitable heuristics) can achieve memory-computation tradeoffs that otherwise justify intervention by an expert. Furthermore, unlike existing static approaches, DTR automatically saves memory on models with arbitrary dynamism, though it began to thrash at lower budgets for LSTM and TreeLSTM. In all cases, the results show that more complex heuristics achieve better memory savings with lower operator overhead, though these complex heuristics also introduce more *runtime* overhead, which must be considered in implementations of DTR. Notably, even the least sophisticated heuristics like LRU (requiring very little runtime overhead) achieved memory savings of up to 30% with very little overhead before thrashing, indicating that some memory savings from checkpointing can be readily obtained.

Limitations. We encountered several illustrative failure modes for DTR in common public implementations of DL models. In PyTorch’s official language model examples [28] and with a popular TreeLSTM implementation [29], a single bottleneck (which turned out to be an encoder or embedding) used over 50% of the baseline memory (not including inputs and weights). Obtaining memory savings in such cases is difficult, as DTR needs to compute the bottleneck while still maintaining an effective checkpointing structure. Notably, a manual PyTorch checkpointing implementation [30] was able to save memory on the language models by splitting the embedding to avoid this bottleneck. We implemented our own versions of these models (closely following the original papers) without such bottlenecks in order to capture the essence of the models’ dynamic structures. These issues would arise in any automatic checkpointing scheme, illustrating that the design of a DL model is a very relevant factor in the applicability of checkpointing techniques.

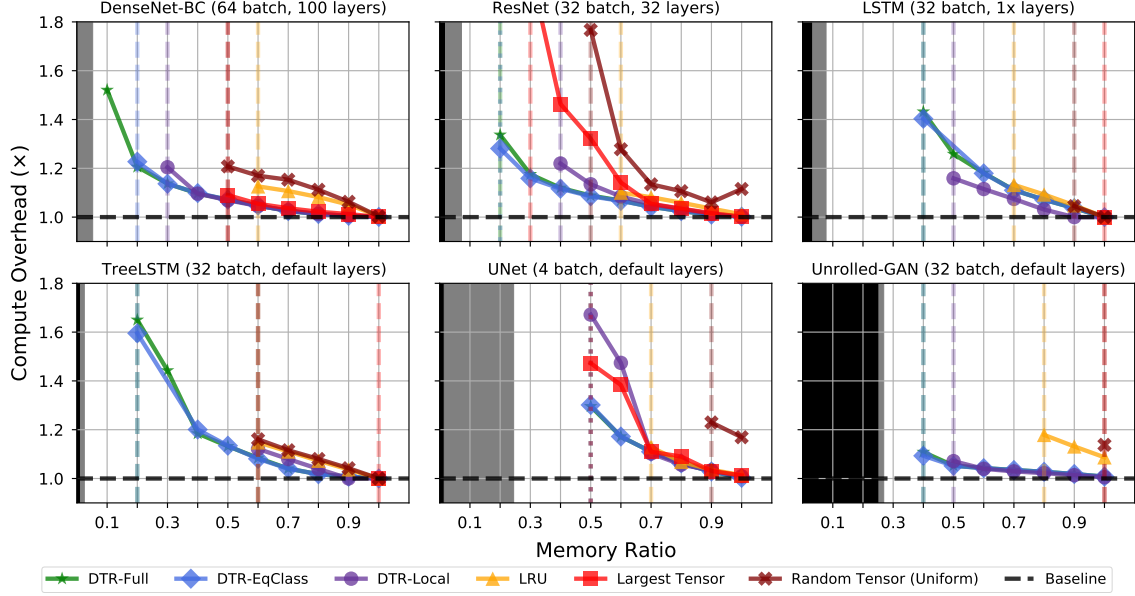


Figure 2: Simulated results comparing different heuristics on various models, comparing rate of computational slowdown for different budgets (fractions of the original peak memory usage). The black area in each graph corresponds to the memory required to store inputs and weights, while the gray area denotes the single operator requiring the most memory to be live at once. The dashed and dotted lines represent the last ratio before thrashing and out-of-memory errors, respectively.

4.2 Prototype Implementation

Following the method of our simulated implementation, we extended our logging mechanism into a prototype DTR implementation in PyTorch⁶ and examined its performance on a variety of models. Our implementation required roughly 2000 lines of C++ additions to PyTorch, roughly half of which were boilerplate for dispatching tensor operations through DTR’s core logic. Based on its favorable performance in the simulated evaluation and the efficiency of its implementation, our prototype used the DTR-EqClass heuristic. Our approach to the implementation avoided making deep modifications to PyTorch’s internal memory management systems or tensor abstractions but resulted in considerable system overhead. Even with the system overhead, the memory savings of this prototype implementation serve as a proof of concept that DTR can be incorporated into DL frameworks without substantial revisions to their core mechanisms.

Comparisons to Unmodified PyTorch. We evaluated the prototype implementation in a manner similar to the simulated trials, using the same models, inputs, and machine, first running unmodified PyTorch to determine the memory required to train a batch of the model and then running the prototype on that model with the budget set to different fractions of the baseline memory.⁷ Due to the lack of publicly available automatic checkpointing implementations for PyTorch, we were unfortunately unable to set up a direct comparison of our prototype with these approaches. As the results in Fig. 3 demonstrate, our prototype is able to save substantial amounts of memory when really executing the models examined in our simulated evaluation. However, the slowdown compared to unmodified PyTorch, even on the full budget (which does not require any evictions), shows that our manner of implementation introduced considerable overhead independent of the tensor operators.

Comparisons on Large Inputs. In addition to these comparisons against the baseline PyTorch implementation, we also assessed the performance of the prototype on model and batch sizes which PyTorch could not fit in our GPU’s physical memory (12 GB), provided in Table 1. We chose ResNet-1202 and TreeLSTM as examples of a static and dynamic model, respectively, for which we could easily increase the input sizes. The peak live memory (ignoring evictions) was 12.5 GB for ResNet-1202 but only 10.1 GB for TreeLSTM (this was also the peak memory of the 10.8GB budget run), which is, in principle, within the GPU’s physical limits — in the latter case, unmodified PyTorch

⁶Publicly available at <https://github.com/uwsaml/dtr-prototype>.

⁷We did not use Unrolled GAN, as it mutates aliases, which would have required much wider modifications to PyTorch to support.

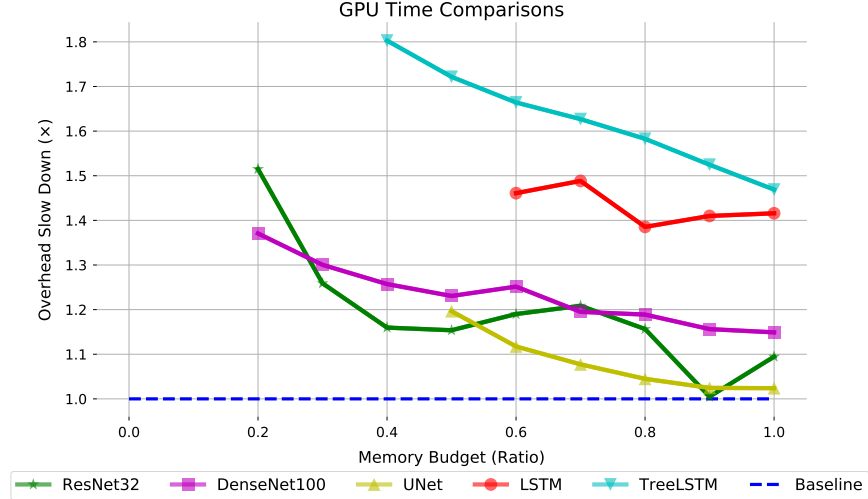


Figure 3: Experimental results for various models on our PyTorch implementation, comparing slowdown relative to unmodified PyTorch (median of 50 trials) as a function of budget (fraction of unmodified PyTorch memory requirement). Datapoints that thrashed ($\geq 2\times$ slowdown) were excluded. The difference between unmodified PyTorch and DTR on the largest budget is primarily due to overhead from the dispatch mechanism.

	10.8GB	9.6GB	8.4GB	6.2GB	5GB	4.8GB	3.6GB	2.4GB	1.2GB	GPU-t
RN	568ms	592ms	610ms	628ms	645ms	660ms	675ms	679ms	742ms	256ms
TL	2.25s	2.50s	2.81s	3.11s	3.48s	3.77s	OOM	OOM	OOM	1.22s

Table 1: Time per batch for ResNet-1202 (RN) and TreeLSTM (TL), median of the averages of 15 iterations across 5 inputs. “OOM” denotes running out of memory. “GPU-t” refers to the time spent on baseline GPU operations only (excluding rematerializations). ResNet-1202 ran on a batch size of 90 on $3 \times 32 \times 32$ images. TreeLSTM ran on a depth 10 binary tree with 100×300 nodes.

likely ran out of memory because of fragmentation and GPU memory required by CuDNN. Note that we could not run on a budget of exactly 12GB because the prototype, for simplicity, only checks whether the budget has been exceeded *after* an allocation, so DTR overallocated in these cases. While these large input sizes had relatively long running times, these were nevertheless able to fit on our GPU’s memory using DTR while they ran out of memory on unmodified PyTorch; indeed, we were able to fit both examples into 40% of the GPU’s physical memory (in ResNet-1202’s case, with less than 50% slowdown compared to the largest budget).

Improving Overhead. While our modifications were kept minimal, they incurred considerable overhead, much of which can likely be attributed to our decision not to modify PyTorch’s core systems. Instead, we introduced an overload layer that results in many more layers of callbacks. The mutation layer also clones tensors (even though it frees the necessary space immediately), resulting in additional overhead. Further modifications to the framework could allow for more optimizations, particularly by reducing the number of heap allocations and conversions between tuples and lists. PyTorch’s define-by-run nature and shallow embedding into Python also meant that much of DTR’s metadata, such as the parent operator of a tensor, needed to be computed at run time (such as by creating a closure). In other frameworks that feature a compilation step [31, 32, 33], it may be possible to eliminate much of this overhead by generating these structures in a compiler pass. We may also note that all the bookkeeping for DTR takes place on CPU while operators are generally offloaded to other devices, so an implementation could interleave these updates with GPU operations.

Profiling also suggests that some overhead came from our heuristic logic, especially searching over the pool of evictable tensors. In order to further reduce the overhead from searching, we added two approximate optimizations to reduce the search space: ignoring small tensors (less than 1% of the average size) and only searching over a random sample of \sqrt{n} tensors from the pool of evictable tensors (for a pool of size n). Even though this improved the search overhead tenfold, searching remains the largest source of DTR-specific overhead. Searching is likely a bottleneck because the implementation recomputes each tensor’s staleness and equivalence class cost upon each eviction, rather than storing and incrementally updating this information. In principle, we can reduce this portion of the overhead by using more complex data structures to maintain an ordering of the tensors to avoid searching, but the additional complexity put it out of scope for a proof-of-concept prototype. Nevertheless, the *relative* slowdowns of the implementation on different

budgets show that the number of additional tensor computations is kept low and that focusing implementation efforts on efficiently maintaining information for heuristics would enable dramatic memory savings.

5 Related Work

Checkpointing in deep learning takes inspiration from checkpointing in reverse-mode AD [4]. Treeverse [34, 5, 35] achieves logarithmic growth in space in exchange for logarithmic growth in computation for programs with statically bounded loops by using a binomial scheme to mark segments of the execution for recomputation. Later AD checkpointing techniques such as those of the Tapenade AD tool [36, 37] and Siskind and Pearlmutter [6] extend Treeverse’s principle to arbitrary programs. However, these techniques produce static plans and impose assumptions about memory usage and cost models. DTR makes fewer assumptions by gathering information at run time and plans dynamically to better utilize available resources, but DTR’s overhead is too large for a general-purpose AD setting, which uses scalar values and operations.

Many DL models can be represented as static dataflow graphs, enabling the straightforward application of Treeverse-like partitioning approaches. Chen *et al.* [8] adapt the ideas of Treeverse to training neural networks by dividing the network into segments to be recomputed during backpropagation, presenting schemes that allow for training an N -layer feedforward network in $\mathcal{O}(\sqrt{N})$ memory with one extra forward pass ($\mathcal{O}(N)$ tensor operations) or in $\mathcal{O}(\log N)$ memory with $\mathcal{O}(N \log N)$ additional tensor operations. The Echo tool [38] also segments a computation graph into subgraphs, but uses cost models for computation and memory to decide which parts of subgraphs should be recomputed rather than recomputing entire segments. Gruslys *et al.* [11] adopt a similar segmenting approach for recurrent neural networks (RNNs) rather than static computation graphs. Other recent work has approached checkpointing in terms of recomputing individual activations rather than segments; several approaches [39, 10, 40] choose values to rematerialize based on the model’s structure, attaining better bounds than Chen *et al.*, while the Checkmate tool [9] reduces the problem to integer linear programming (ILP).

DTR differs fundamentally from prior approaches to checkpointing in DL in that it handles arbitrary dynamic control flow in models (making no assumptions about the model’s structure) and operates online, giving it access to dynamically gathered information. In principle, a static checkpointing technique could be applied to a dynamic model “just in time” by unrolling the model on the fly, but some static analyses (like Checkmate’s ILP solver) can be too expensive to run each epoch. Unlike static approaches, however, dynamic planning does have the constraint of also managing overhead at run time, which limits the analysis DTR’s heuristics can feasibly perform.

Note that Chen *et al.*’s greedy segmentation scheme and the GreedyRemat baseline from Kumar *et al.* [10] are similar to DTR in that they greedily place checkpoints using a heuristic. However, these algorithms assume a topologically sorted static graph and their heuristics only use the sizes of tensors.

6 Conclusion

DTR provides a simple, customizable approach to checkpointing for DL models that supports a very general range of applications without manual annotation or modifications to applications. Our simulations show that DTR achieve favorable memory-computation tradeoffs on both static and dynamic models, despite lacking any advance knowledge of a model’s behavior. The prototype achieves real memory savings and demonstrates that DTR can support many implementation details of DL frameworks, which we hope will spur the adoption of similar techniques in practice.

The memory savings demonstrated suggest avenues of further investigation. For example, DTR could leverage further sources of information that may improve performance, such as by learning from past batches or applying static analyses to input programs. The simplicity of DTR’s core design invites further modifications and exploration to suit the varying demands of applications, including more varied training tasks, distributed settings, and low-powered devices.

7 Broader Impacts

Checkpointing can help train DL models on devices whose memory constraints would otherwise be preventative or using batch sizes that would otherwise be too large. Past checkpointing techniques have generally been restricted to static models and thus have not uniformly benefited all DL applications. By supporting arbitrary models, DTR removes barriers for checkpointing more dynamic models used in application areas like natural language processing (NLP).

Access to increasingly large and expensive accelerators, *e.g.*, the most recent GPUs, has also been a significant force driving DL research for the past decade. While such devices have enabled tremendous progress, their expense has also shaped what questions the DL community investigates, which groups are able to conduct such research, and contributed

to hazardous technological waste as the previous generation of GPUs quickly becomes obsolete. DTR presents the potential for a new way to explore more DL research questions on more-affordable devices. On one hand, we hope this will enable more teams to join the DL research community by eliminating barriers to entry based on limited access to computational resources, and to promote more environmentally friendly hardware reuse. On the other hand, any improvement to DL efficiency or applicability may contribute to economic and privacy concerns arising from increased technology company monopolization as discussed in Zuboff’s *The Age of Surveillance Capitalism* [41].

We also see opportunities for DTR to build bridges between the DL, Programming Languages (PL), and Computer Architecture (Arch) communities. DTR has close ties to garbage collection techniques from the PL literature [42], and modern accelerators being developed in the Arch community are often memory-constrained [9, 43]. DTR provides a flexible framework where ideas and voices from these communities can collaborate. While increased collaboration is an exciting opportunity, there is also the possibility that moving more researchers toward DL will deprive society of significant investigations in other important research areas.

Acknowledgements

This work was supported by the Applications Driving Architectures (ADA) Research Center, a JUMP Center co-sponsored by SRC and DARPA. The Titan V used for this research was donated by the NVIDIA Corporation. We would also like to thank Eunice Jun and Josh M. Pollock for providing feedback and useful comments on various drafts of this work.

References

- [1] Tom B. Brown, Benjamin Mann, Nick Ryder, Melanie Subbiah, Jared Kaplan, Prafulla Dhariwal, Arvind Nee-lakantan, Pranav Shyam, Girish Sastry, Amanda Askell, Sandhini Agarwal, Ariel Herbert-Voss, Gretchen Krueger, Tom Henighan, Rewon Child, Aditya Ramesh, Daniel M. Ziegler, Jeffrey Wu, Clemens Winter, Christopher Hesse, Mark Chen, Eric Sigler, Mateusz Litwin, Scott Gray, Benjamin Chess, Jack Clark, Christopher Berner, Sam McCandlish, Alec Radford, Ilya Sutskever, and Dario Amodei. Language models are few-shot learners, 2020.
- [2] Jacob Devlin, Ming-Wei Chang, Kenton Lee, and Kristina Toutanova. Bert: Pre-training of deep bidirectional transformers for language understanding, 2018.
- [3] Andrew Brock, Jeff Donahue, and Karen Simonyan. Large scale gan training for high fidelity natural image synthesis, 2018.
- [4] Atilim Gunes Baydin, Barak A. Pearlmutter, Alexey Andreyevich Radul, and Jeffrey Mark Siskind. Automatic differentiation in machine learning: a survey. *CoRR*, abs/1502.05767, 2015.
- [5] Andreas Griewank and Andrea Walther. Treeverse: An implementation of checkpointing for the reverse or adjoint mode of computational differentiation. 03 1998.
- [6] Jeffrey Mark Siskind and Barak A. Pearlmutter. Divide-and-conquer checkpointing for arbitrary programs with no user annotation. *Optimization Methods and Software*, 33(4-6):1288–1330, Sep 2018.
- [7] Nimit Sharad Sohoni, Christopher Richard Aberger, Megan Leszczynski, Jian Zhang, and Christopher Ré. Low-memory neural network training: A technical report. *CoRR*, abs/1904.10631, 2019.
- [8] Tianqi Chen, Bing Xu, Chiyuan Zhang, and Carlos Guestrin. Training deep nets with sublinear memory cost. *CoRR*, abs/1604.06174, 2016.
- [9] Paras Jain, Ajay Jain, Aniruddha Nrusimha, Amir Gholami, Pieter Abbeel, Joseph Gonzalez, Kurt Keutzer, and Ion Stoica. Checkmate: Breaking the memory wall with optimal tensor rematerialization. In *Proceedings of Machine Learning and Systems 2020*, pages 497–511, 2020.
- [10] Ravi Kumar, Manish Purohit, Zoya Svitkina, Erik Vee, and Joshua Wang. Efficient rematerialization for deep networks. In H. Wallach, H. Larochelle, A. Beygelzimer, F. dAlché Buc, E. Fox, and R. Garnett, editors, *Advances in Neural Information Processing Systems 32*, pages 15172–15181. Curran Associates, Inc., 2019.
- [11] Audrunas Gruslys, Rémi Munos, Ivo Danihelka, Marc Lanctot, and Alex Graves. Memory-efficient backpropagation through time. *CoRR*, abs/1606.03401, 2016.
- [12] Kai Sheng Tai, Richard Socher, and Christopher D. Manning. Improved semantic representations from tree-structured long short-term memory networks. *Proceedings of the 53rd Annual Meeting of the Association for Computational Linguistics and the 7th International Joint Conference on Natural Language Processing (Volume 1: Long Papers)*, 2015.

- [13] Jiayuan Mao, Chuang Gan, Pushmeet Kohli, Joshua B. Tenenbaum, and Jiajun Wu. The neuro-symbolic concept learner: Interpreting scenes, words, and sentences from natural supervision, 2019.
- [14] Kenton Lee, Mike Lewis, and Luke Zettlemoyer. Global neural CCG parsing with optimality guarantees. *CoRR*, abs/1607.01432, 2016.
- [15] Chelsea Finn, Pieter Abbeel, and Sergey Levine. Model-agnostic meta-learning for fast adaptation of deep networks. *CoRR*, abs/1703.03400, 2017.
- [16] Luke Metz, Ben Poole, David Pfau, and Jascha Sohl-Dickstein. Unrolled generative adversarial networks. 2017.
- [17] Adam Paszke, Sam Gross, Francisco Massa, Adam Lerer, James Bradbury, Gregory Chanan, Trevor Killeen, Zeming Lin, Natalia Gimelshein, Luca Antiga, Alban Desmaison, Andreas Köpf, Edward Yang, Zach DeVito, Martin Raison, Alykhan Tejani, Sasank Chilamkurthy, Benoit Steiner, Lu Fang, Junjie Bai, and Soumith Chintala. Pytorch: An imperative style, high-performance deep learning library, 2019.
- [18] Preston Briggs, Keith D. Cooper, and Linda Torczon. Rematerialization. In *Proceedings of the ACM SIGPLAN 1992 Conference on Programming Language Design and Implementation, PLDI '92*, page 311–321, New York, NY, USA, 1992. Association for Computing Machinery.
- [19] John Binder, Kevin P. Murphy, and Stuart J. Russell. Space-efficient inference in dynamic probabilistic networks. In *IJCAI*, 1997.
- [20] Olivier Beaumont, Julien Herrmann, Guillaume Pallez, and Alena Shilova. Optimal memory-aware backpropagation of deep join networks. *Philosophical Transactions of the Royal Society A: Mathematical, Physical and Engineering Sciences*, 378, 01 2019.
- [21] Adam Paszke, Sam Gross, Soumith Chintala, Gregory Chanan, Edward Yang, Zachary DeVito, Zeming Lin, Alban Desmaison, Luca Antiga, and Adam Lerer. Automatic differentiation in pytorch. 2017.
- [22] Kaiming He, Xiangyu Zhang, Shaoqing Ren, and Jian Sun. Deep residual learning for image recognition. *CoRR*, abs/1512.03385, 2015.
- [23] Gao Huang, Zhuang Liu, Laurens Van Der Maaten, and Kilian Q. Weinberger. Densely connected convolutional networks. *2017 IEEE Conference on Computer Vision and Pattern Recognition (CVPR)*, Jul 2017.
- [24] Olaf Ronneberger, Philipp Fischer, and Thomas Brox. U-net: Convolutional networks for biomedical image segmentation. *Medical Image Computing and Computer-Assisted Intervention – MICCAI 2015*, page 234–241, 2015.
- [25] Sepp Hochreiter and Jürgen Schmidhuber. Long short-term memory. *Neural Comput.*, 9(8):1735–1780, November 1997.
- [26] Kai Sheng Tai, Richard Socher, and Christopher D. Manning. Improved semantic representations from tree-structured long short-term memory networks. *CoRR*, abs/1503.00075, 2015.
- [27] Geoff Pleiss, Danlu Chen, Gao Huang, Tongcheng Li, Laurens van der Maaten, and Kilian Q. Weinberger. Memory-efficient implementation of densenets. https://github.com/gpleiss/efficient_densenet_pytorch, 2017.
- [28] PyTorch Team. Word-level language modeling rnn. https://github.com/pytorch/examples/tree/master/word_language_model, 2020.
- [29] Riddhiman Dasgupta. treelstm.pytorch. <https://github.com/dasguptar/treelstm.pytorch>, 2018.
- [30] Trading compute for memory in pytorch models using checkpointing. https://github.com/prigoyal/pytorch_memonger/blob/master/tutorial/Checkpointing_for_PyTorch_models.ipynb, 2017.
- [31] Nadav Rotem, Jordan Fix, Saleem Abdulrasool, Summer Deng, Roman Dzhabarov, James Hegeman, Roman Levenstein, Bert Maher, Satish Nadathur, Jakob Olesen, Jongsoo Park, Artem Rakhov, and Misha Smelyanskiy. Glow: Graph lowering compiler techniques for neural networks. *CoRR*, abs/1805.00907, 2018.
- [32] Jared Roesch, Steven Lyubomirsky, Marisa Kirisame, Josh Pollock, Logan Weber, Ziheng Jiang, Tianqi Chen, Thierry Moreau, and Zachary Tatlock. Relay: A high-level IR for deep learning. *CoRR*, abs/1904.08368, 2019.
- [33] Chris Lattner, Mehdi Amini, Uday Bondhugula, Albert Cohen, Andy Davis, Jacques Pienaar, River Riddle, Tatiana Shpeisman, Nicolas Vasilache, and Oleksandr Zinenko. Mlir: A compiler infrastructure for the end of moore’s law, 2020.
- [34] Andreas Griewank. Achieving logarithmic growth of temporal and spatial complexity in reverse automatic differentiation. *Optimization Methods and Software*, 1, 04 1994.

- [35] Andreas Griewank and Andrea Walther. Algorithm 799: Revolve: An implementation of checkpoint for the reverse or adjoint mode of computational differentiation. *ACM Transactions on Mathematical Software*, 26(1):19–45, mar 2000.
- [36] Laurent Hascoet and Mauricio Araya-Polo. Enabling user-driven checkpointing strategies in reverse-mode automatic differentiation, 2006.
- [37] Laurent Hascoet and Valérie Pascual. The tapenade automatic differentiation tool: Principles, model, and specification. *ACM Trans. Math. Softw.*, 39(3), May 2013.
- [38] Bojian Zheng, Abhishek Tiwari, Nandita Vijaykumar, and Gennady Pekhimenko. Echo: Compiler-based gpu memory footprint reduction for lstm rnn training, 2018.
- [39] Mitsuru Kusumoto, Takuya K Inoue, Gentaro Watanabe, Takuya Akiba, and Masanori Koyama. A graph theoretic framework of recomputation algorithms for memory-efficient backpropagation. In *NeurIPS*, 2019.
- [40] Julien Herrmann, Olivier Beaumont, Lionel Eyraud-Dubois, Julien Hermann, Alexis Joly, and Alena Shilova. Optimal checkpointing for heterogeneous chains: how to train deep neural networks with limited memory, 2019.
- [41] Shoshana Zuboff. *The Age of Surveillance Capitalism: The Fight for a Human Future at the New Frontier of Power*. 1st edition, 2018.
- [42] Richard Jones, Antony Hosking, and Eliot Moss. *The Garbage Collection Handbook: The Art of Automatic Memory Management*. Chapman & Hall/CRC, 1st edition, 2011.
- [43] Norman P. Jouppi, Cliff Young, Nishant Patil, David Patterson, Gaurav Agrawal, Raminder Bajwa, Sarah Bates, Suresh Bhatia, Nan Boden, Al Borchers, Rick Boyle, Pierre-luc Cantin, Clifford Chao, Chris Clark, Jeremy Coriell, Mike Daley, Matt Dau, Jeffrey Dean, Ben Gelb, Tara Vazir Ghaemmaghami, Rajendra Gottipati, William Gulland, Robert Hagmann, C. Richard Ho, Doug Hogberg, John Hu, Robert Hundt, Dan Hurt, Julian Ibarz, Aaron Jaffey, Alek Jaworski, Alexander Kaplan, Harshit Khaitan, Daniel Killebrew, Andy Koch, Naveen Kumar, Steve Lacy, James Laudon, James Law, Diemthu Le, Chris Leary, Zhuyuan Liu, Kyle Lucke, Alan Lundin, Gordon MacKean, Adriana Maggiore, Maire Mahony, Kieran Miller, Rahul Nagarajan, Ravi Narayanaswami, Ray Ni, Kathy Nix, Thomas Norrie, Mark Omernick, Narayana Penukonda, Andy Phelps, Jonathan Ross, Matt Ross, Amir Salek, Emad Samadiani, Chris Severn, Gregory Sizikov, Matthew Snelham, Jed Souter, Dan Steinberg, Andy Swing, Mercedes Tan, Gregory Thorson, Bo Tian, Horia Toma, Erick Tuttle, Vijay Vasudevan, Richard Walter, Walter Wang, Eric Wilcox, and Doe Hyun Yoon. In-datacenter performance analysis of a tensor processing unit. In *Proceedings of the 44th Annual International Symposium on Computer Architecture, ISCA '17*, page 1–12, New York, NY, USA, 2017. Association for Computing Machinery.

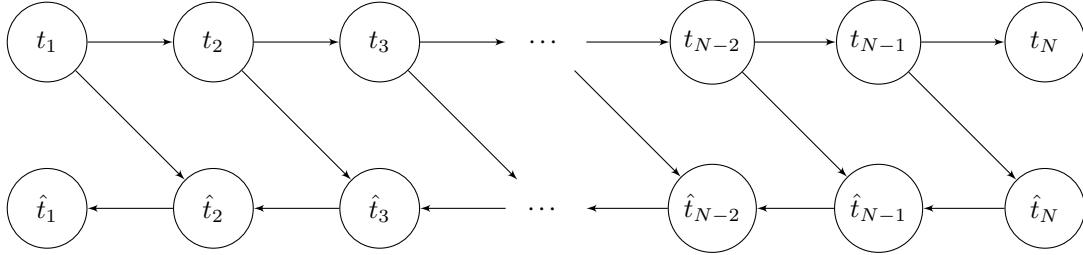
A Proof of Theorem 3.1

In this section, we provide a proof of the $\mathcal{O}(N)$ runtime of DTR on a linear feed-forward network with uniform operator compute and memory cost, under a reduced heuristic. We begin with a thorough treatment of the network architecture, and then motivate our reduced heuristic h_{e^*} in this simplified setting. Finally, we prove Theorem 3.1.

A.1 Network Definition

We assume the network consists of operators f_1, \dots, f_N , where the tensor computed by the i th operator is given by $f_i(t_{i-1})$, with t_j denoting the tensor computed by the j th operator. Note that we consider t_0 to be the input tensor, which for simplicity will always reside in memory and not contribute to the active memory consumption. For this reason, we may consider f_1 to be a nullary operator. Additionally, we assume that the size of each tensor (denoted $\text{size}(t)$) is 1, and likewise for the compute time $c(f_i)$ for each operator f_i . Note that we may write $c(f_t)$ to mean the same as $c(f_i)$ for $t = t_i$, when the index i is not convenient.

For backpropagation, we assume each operator f_i has an associated *gradient* operator \hat{f}_i , which computes the result $\hat{t}_i = \hat{f}_i(t_{i-1}, \hat{t}_{i+1})$. We may consider $\hat{t}_{N+1} = 1$ to be an unevictable unit tensor, as is the case in automatic differentiation, but for simplicity we define $\hat{t}_1 = \hat{f}_1(\hat{t}_2)$ and $\hat{t}_N = \hat{f}_N(t_{N-1})$. As above, we assume unit memory and compute for each \hat{f}_i .



A.2 Liveness and Banishing

To optimize memory usage during computation, we introduce the notion of *liveness* and *banishing*. At a high level, liveness allows us to determine when a given tensor is no longer required for subsequent network computations, which in turn allows us to permanently free (banish) tensors to regain memory when certain conditions are met.

To be more precise, we formalize the network as a program:

```

let t1 := f1();
let t2 := f2(t1);
...
let tN := fN(t_{N-1});
// Backpropagate.
let t_hat_N := f_hat_N(t_{N-1});
let t_hat_{N-1} := f_hat_{N-1}(t_{N-2}, t_hat_N);
...
let t_hat_2 := f_hat_2(t1, t_hat_3);
let t_hat_1 := f_hat_1(t_hat_2);

```

We say a tensor t is *live* when there is a pending operation in the program that takes t as an input. When t is no longer live, *and* every tensor directly computed using t is in memory or banished, then we say t is *banished* and we reclaim the memory used by t . Banishing a tensor additionally makes its children unevictable.

Thus for example, t_N can be immediately banished after computing, t_{N-1} can be banished after \hat{t}_N , both t_{N-2} and \hat{t}_N after \hat{t}_{N-1} , and so on. This will become important in the proof.

The analysis of liveness can be done statically for static models, and by reference counting for models with dynamism.

A.3 Heuristic Definition

Heuristic h_{e^*} is a reduced form of the DTR heuristic, as it does not account for tensor staleness. Here, we provide a detailed motivation of its definition.

Recall the *evicted neighborhood* $e^*(t)$ of tensor t , as described in Section 3 and further formalized in Appendix C.2.

Definition A.1 (Rematerialization Compute Cost). For a given tensor t , the *rematerialization compute cost* of t is the value

$$c^*(t) = \sum_{t' \in e^*(t)} c(f_{t'})$$

Now, we define the reduced heuristic in full generality; the definition of h_{e^*} will be a consequence of the simplified setting we analyze.

Definition A.2 (Compute-Memory Heuristic (general)). The *compute-memory* heuristic score for a material tensor t is defined as

$$h_{e^*}(t) = \frac{c^*(t) + c(f_t)}{\text{size}(t)}$$

Corollary A.1. *Under our simplified compute and memory constraints, $h_{e^*}(t) = |e^*(t)| + 1$. Since the heuristic is only used to rank tensors, the common additive constant 1 is unimportant. The heuristic $|e^*(t)|$ will have the same behavior as $|e^*(t)| + 1$.*

Note importantly that uncomputed tensors are not considered in any of the above definitions (as we do not know about their existence yet, from a dynamic execution perspective).

A.4 Proof of Theorem 3.1

Now we prove Theorem 3.1, which bounds the overhead of DTR on a linear feedforward network with N nodes and \sqrt{N} memory by a constant factor of the runtime required by an algorithm with unlimited memory.

Proof. To prove this claim, we will consider the forward pass and the backward pass separately. In the forward pass, we show that our algorithm only performs N computations, matching that of an algorithm with unlimited memory. Furthermore, upon completion of the forward pass, we tightly characterize the B tensors that remain in memory. We show that a set of evenly spaced *checkpoint tensors* remain in memory throughout the backward pass, until banishment. The presence of these checkpoint tensors allows us to argue that the algorithm never has to rematerialize too many tensors in a row. Furthermore, as the algorithm computes additional gradients, it banishes checkpoint tensors that are no longer needed, freeing more space for additional checkpoints. The overhead incurred by the algorithm can therefore be kept to a constant factor of the required $\Theta(N)$ time. This checkpointing behavior can be seen in the trace of the algorithm, visualized in Figure 4.

We now analyze each of the phases in detail.

Phase 1: Forward pass

Recall that in a feed-forward network, every computation depends only on the preceding one. Thus in our simplified network, we only ever need $B = 2$ units of memory to compute the forward pass without any rematerializations (furthermore, this is the minimum required memory). For this reason, the forward pass requires N computations.

After completing the forward pass, we can tightly characterize the tensors remaining in memory. In particular, Lemma A.1 tells us that the maximum gap between material tensors is bounded by

$$L \leq \frac{2(N-2)}{B-1}$$

We note that this bound is tight in an asymptotic sense: if we can keep B tensors in memory, and the forward pass is of length N , then the maximum gap must be at least N/B .

Next, we will analyze the backward pass. Key to this analysis is the claim that “not too many” of the tensors in memory at the beginning of the forward pass are evicted before banishment during the backward pass. The existence of these “checkpoint tensors” allows us to argue that we do not do too much rematerialization work.

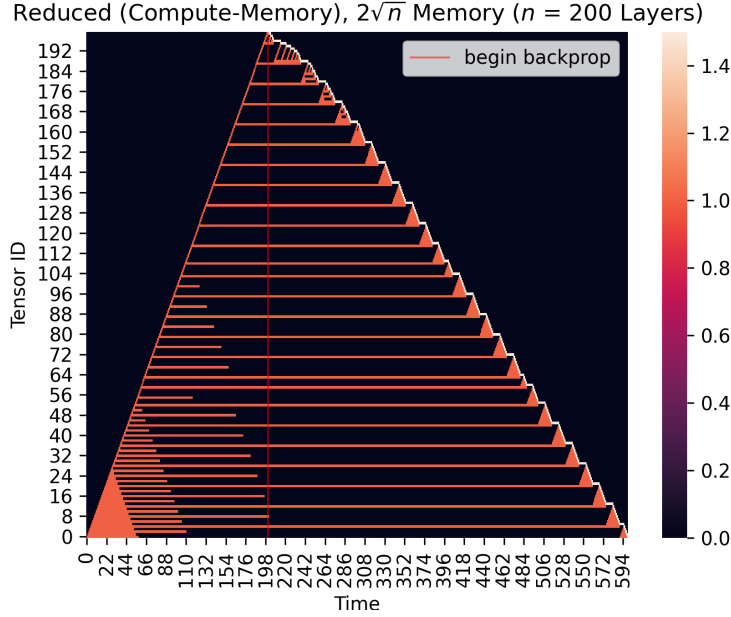


Figure 4: Visualization of the state of memory for DTR with $N = 200$, $B = 2\lceil\sqrt{N}\rceil$, and heuristic h_{e^*} . A value of 0 (black) indicates the tensor is evicted or banished, 1 (red) indicates the tensor is a forward value in memory, and 1.5 (white) denotes an in-memory gradient tensor corresponding to the forward tensor. The backward pass begins at the red vertical line; note the presence of evenly spaced *checkpoint tensors* (red horizontal lines) that persist in memory throughout the backward pass. Note also the recursive checkpointing behavior visible in the early gaps of the backward pass, and finally the completely red triangles of the later gaps, when there is enough free memory to avoid repeated rematerialization altogether.

Phase 2: Backward pass

During the backward pass, our algorithm computes gradients \hat{t}_i . Each gradient computation relies on two inputs: \hat{t}_{i+1} and t_{i-1} . We show that neither input incurs too much rematerialization cost - \hat{t}_{i+1} because it is pinned in memory, and t_{i-1} because the paths of immaterial tensors are not “too long.” The first condition follows from the fact that t_i is banished after computing \hat{t}_{i+1} , therefore forcing \hat{t}_{i+1} to remain in memory until it is banished. The second condition is formalized in the following lemma, proved later in this section.

Lemma A.1 (Checkpointing). *Consider an execution of the DTR algorithm with B units of memory and heuristic h_{e^*} , applied to the graph described in section A.1. Let S be the set of tensors in memory after computation of t_N in the forward pass. Then, $C \subseteq S$ is a set of “checkpoint” tensors from the forward pass with the following properties:*

1. *During the backward pass, each $c \in C$ stays in memory until it is banished.*
2. *The gap between neighboring tensors in C satisfies*

$$L \leq \frac{4(N-2)}{B-1}$$

These $|C|$ checkpoint tensors divide the n forward tensors into $|C|$ groups, indexed by k , each of length $L_k \leq \frac{4(N-2)}{B-1}$. The total computational cost of the backward pass is equal to the sum of the computational cost for each group,

$$C = \sum_{k=1}^{|C|} C_k.$$

The second key insight in the analysis of the backward pass is that, for every group that is processed, the algorithm banishes a checkpoint tensor $c \in C$ and receives a unit of extra memory. In particular, at the start of processing group

$|C| - k$, the algorithm has $2 + k$ pieces of extra memory (two from banishing the most recently used gradient and forward tensor, and k from the banished checkpoint tensors). We can leverage this extra memory to process the gradients in later groups with less rematerialization overhead, using the k extra units of memory to create intermediate checkpoint tensors. The following lemma describes how the cost of computing all the gradients in a group decreases as we free more memory.

Lemma A.2. *Suppose we have $2 + k$ pieces of free memory to compute all of the gradients associated with an immaterial forward tensor path of length L_k . Then the number of rematerializations needed to compute all the gradients is of order*

$$C_k = \mathcal{O} \left(L_k + \frac{L_k^2}{k^2} \log k \right)$$

Applying this lemma, the total cost of the backward pass becomes

$$\begin{aligned} C &= \sum_{k=1}^{|C|} C_k \\ &\lesssim \sum_{k=1}^{|C|} \left(L_k + \frac{L_k^2}{k^2} \log k \right) \\ &\leq \sum_{k=1}^{|C|} L_k + \sum_{k=1}^{|C|} \frac{\log k}{k^2} L_k^2 \\ &\leq |C| \left(\frac{4(N-2)}{B-1} + 1 \right) + \sum_{k=1}^{|C|} \frac{\log k}{k^2} \left(\frac{4(N-2)}{B-1} + 1 \right)^2 \\ &\lesssim |C| \left(\frac{N}{B} \right) + \frac{N^2}{B^2} \sum_{k=1}^{|C|} \frac{\log k}{k^2} \end{aligned}$$

where \lesssim hides constant factors. Note that $|C| \leq B$, since $C \in S$ where S is the set of tensors in memory at the end of the forward pass. Also note that $\frac{\log k}{k^2}$ is a convergent sequence, so its partial sums are bounded. Therefore, we can simplify the bound to

$$C \lesssim N + \frac{N^2}{B^2}$$

Since $B = \Omega(\sqrt{N})$, we conclude that the total cost of the backward pass is $\mathcal{O}(N)$. Adding this to the $\mathcal{O}(N)$ cost of the forward pass, we see the total compute is $\mathcal{O}(N)$, as desired. \square

A.5 Proofs of Intermediate Results

Here, we present intermediate results that we used in the proof of our main result.

Lemma A.3. *Consider the DTR algorithm operating with heuristic h_{e^*} . Suppose we seek to (re)materialize forward tensor t_k for $k \leq N$, where the material tensor preceding t_k is denoted by t_j (with $j < k$). Suppose also that t_j is not evicted during the computation of t_k . Then, if the algorithm begins with t_j in memory and with M units of memory, and runs until computing t_k , then the maximum length L of any evicted sequence of tensors between t_j and t_k is bounded by*

$$L \leq 2((k-j)-1)/(M-1)$$

Proof. Proof by induction. We will show that, when the algorithm computes tensor $j+i$, for $i = 1, 2, \dots, k-j$, the maximum length of an evicted sequence of tensors between t_j and t_{j+i} satisfies

$$L_i \leq 2(i-1)/(M-1)$$

Base case. When $i = 1$, both t_j and $t_{j+1} = t_k$ are material tensors, so the gap is $L_1 = 0$.

Inductive step. Consider the contents of memory after computing t_{j+i} . We begin by partitioning tensors t_j, \dots, t_{j+i} into M segments S_1, \dots, S_M , each ending in a material tensor (note, the last segment must end on a material tensor,

since t_{j+i} was just computed). If $i < M$ so that there are not M material tensors, then the length of each segment is zero and we are done. Otherwise, each segment corresponds to an evicted sequence of zero or more tensors (i.e., the tensors preceding the material tensor). Let s_i denote the material tensor that ends segment i .

Now, consider all adjacent pairs of segments (S_l, S_{l+1}) for $1 \leq l \leq M-1$. The average length of the pairs is given by

$$\begin{aligned} \bar{L} &= \sum_{l=1}^{M-1} \frac{|S_l| + |S_{l+1}|}{M-1} \\ &= \left(2 \sum_{l=1}^M \frac{|S_l|}{M-1} \right) - \frac{|S_1| + |S_M|}{M-1} \\ &= \frac{2}{M-1} \left(\sum_{l=1}^M |S_l| \right) - \frac{|S_1| + |S_M|}{M-1} \\ &= \frac{2i}{M-1} - \frac{|S_1| + |S_M|}{M-1} \\ &\leq \frac{2(i-1)}{M-1}. \end{aligned}$$

Let $(S_{l'}, S_{l'+1})$ be the pair of adjacent segments with minimum combined length. Since the average length is bounded by the inequality above, it follows that the length of $(S_{l'}, S_{l'+1})$ is also less than or equal to $2(i-1)/(M-1)$.

Since the heuristic evicts the tensor that results in the smallest gap, we conclude that the eviction will create a gap no larger than $2(i-1)/(M-1)$. By the inductive hypothesis, the largest previous gap was no larger than $2(i-2)/(M-1)$, so we conclude that the largest gap after this computation is no more than $2(i-1)/(M-1)$. \square

Proof of Lemma A.1

Proof. We will prove this lemma by dividing the backward pass into two phases. In the first phase, the first two gradient computations of the backward pass, we may be forced to evict some element of S . In the absence of further information on the evicted tensor, we upper bound the resulting gap by twice the maximum gap between tensors in S . This gives us the upper bound in Item 2 of the lemma.

In the second phase, the remaining $N-2$ gradient computations of the backward pass, we show that heuristic h_{e^*} never leads us to evict a tensor that would lead to a gap of more than $\frac{4(N-2)}{B-1}$ among the tensors in memory. This allows us to conclude that the checkpoint tensors C remain in memory until eviction, as claimed.

We now elaborate on the two phases, as discussed above.

Phase 1: The first two gradient computations of the backward pass.

We present a detailed treatment of the first two gradient computations in the backward pass, \hat{t}_N and \hat{t}_{N-1} . We will show that, during the course of these two computations, at most one tensor from S is evicted from memory. Since Lemma A.3 tells us that the maximum gap in S satisfies $L_S \leq \frac{2(N-2)}{B-1}$, we conclude that removing a single tensor results in a gap in C of no more than $2L_S$. Additionally, we will show that after the computation of the first two gradients, there are at least two non-checkpoint tensors in memory. Since only two free units of memory are required to rematerialize a path of tensors, this sets us up for the analysis of the remaining gradient computations.

We begin by noting that, after the forward pass completes, t_N and t_{N-1} are both in memory (since t_N has just been computed, which requires t_{N-1}). Since t_N is no longer needed in subsequent computations, it is immediately banished. Assuming $B \leq N$, this leaves us with exactly one unit of free memory (if $B > N$, no elements of S are banished in the first two computations, and the $2L_s$ bound is trivial). This single unit of memory is then filled by the computation of \hat{t}_N , which only depends on t_{N-1} .

Now, t_{N-1} is no longer needed, so it is banished, and we have exactly one unit of free memory. To compute \hat{t}_{N-1} , we require t_{N-2} and \hat{t}_N to be in memory. Since \hat{t}_N was just computed, it is clearly in memory. However, t_{N-2} may or may not be in memory. We consider the two cases separately.

If t_{N-2} is in memory, then we immediately compute \hat{t}_{N-1} . Next, tensors t_{N-2} and \hat{t}_N are banished, leaving us with the desired two free units of memory.

If, on the other hand, t_{N-2} is not in memory, we must rematerialize it. Let t_j be the material tensor that terminates the immaterial path of tensors containing t_{N-2} . We need to perform the sequence of computations $\{t_{j+1}, t_{j+2}, \dots, t_{N-2}\}$. However, we only have one unit of free memory, so after computing t_{j+1} we will need to evict some tensor from memory. The evicted tensor must be t_i for some $i \leq j$, as neither t_{j+1} nor t_N can be evicted (the former will be used for the next computation, and the latter is pinned in memory).

Regardless of which tensor t_i is evicted, the length of the immaterial path it creates cannot exceed $2L_S$, where L_S is the length of the longest path in S . Lemma A.3 bounds $L_S \leq \frac{2(N-2)}{B-1}$, so this step of the algorithm maintains Item 2 of the lemma.

It remains to show that the maximum gap in \mathcal{C} does not become larger than $2L_S$ during the remaining steps of rematerialization, and that the computation of \hat{t}_{N-1} ends with at least two units of free memory. To show the first claim, we note that the number of immaterial tensors on the path to \hat{t}_{N-1} does not exceed $2L_S$ (this is the maximum length possible, if t_j was evicted and its adjacent immaterial paths were both of length L_S). Therefore, when performing the intermediate rematerializations necessary to rematerialize t_{N-2} , it is always possible to evict a tensor between t_j and t_{N-2} , with a heuristic value of less than $2L_S$. Since we evict the tensor with the smallest heuristic value, we will never create an immaterial path of length greater than $2L_S$.

Finally, we note that, after computing \hat{t}_{N-1} , both t_{N-2} and \hat{t}_N will be banished. This leaves us with the desired two units of free memory.

We have shown that, after computing \hat{t}_{N-1} , the algorithm has two units of free memory, and the checkpoint set \mathcal{C} has a maximum gap of no more than $2L_S$. Next, we show that this set \mathcal{C} is maintained throughout the remainder of the backward pass.

Phase 2: The remaining $N - 2$ gradient computations.

The analysis for the remainder of the backward pass follows via induction, using the argument for rematerializing t_{N-2} above.

We have already shown a base case; we can maintain the desired properties of \mathcal{C} when computing \hat{t}_{N-2} . For the inductive step, consider the computation of \hat{t}_i for $1 < i < N - 1$. Suppose we have at least two units of free memory, and \hat{t}_{i+1} in memory. Furthermore, suppose that the set \mathcal{C} satisfies the properties of the lemma. We need to rematerialize t_{i-1} , which terminates a path of immaterial tensors of length no more than $2L_S$. As we rematerialize this path, it may require evicting tensors from memory. However, by the same logic we applied above, we know that the algorithm may always choose to evict a tensor resulting in a path of less than $2L_S$. The algorithm will always choose this option in favor of creating a longer immaterial path. We conclude that the upper bound of $2L_S$ is preserved when computing \hat{t}_i . Furthermore, after \hat{t}_i is computed, we may evict \hat{t}_{i+1} and t_{i-1} , giving us two units of free memory. This proves the inductive step.

Note that, in the case that $i = 1$, the computation requires no rematerializations, as \hat{t}_1 only depends on \hat{t}_2 , and the latter is in memory at the time of computing \hat{t}_1 . \square

Proof of Lemma A.2

Proof. Let $C_{i,k}$ denote the cost of processing gradient i in this group. Since there are L_k associated gradients, the total cost is

$$C_k = \sum_{i=1}^{L_k} C_{i,k}.$$

To compute each $C_{i,k}$ we note that computation of the gradients proceeds in phases. When the first gradient is computed (at cost $C_{0,k} = L_k$), two units of memory must be devoted to the current tensor computation, while the remaining k units of memory are used for intermediate rematerialized tensors. Applying the intermediate checkpointing lemma, A.4, we conclude that some of these intermediate tensors will remain as checkpoints (indexed by j , with $j = 1$ indicating the highest-indexed tensor), with adjacent checkpoints separated by a distance at most $L_{k,j} = \frac{4(L_k-2)}{k-1}$. We can express the total cost of computing the gradients in this gap as

$$C_k = L_k + \sum_j \sum_{i \in \text{group } j} C_{i,k}$$

We begin by considering the first group to be processed, $j = 1$, associated with the last path between checkpoints. Since it is the first group to be processed, it has no spare memory for intermediate checkpoints. Therefore, computing the first gradient requires rematerializing the entire group (with at most $L_{k,j}$ intermediate tensors), computing the second gradient requires rematerializing at most $L_{k,j} - 1$ tensors, and so on. This gives a total cost bounded as follows (using \lesssim to denote inequality up to constant factors).

$$\begin{aligned} \sum_{i \in \text{group } 1} C_{i,k} &\leq \sum_{l=0}^{L_{k,j}} L_{k,j} - l \\ &\lesssim (L_{k,j})^2 \\ &= \left(\frac{4(L_k - 2)}{k - 1} + 1 \right)^2 \\ &\lesssim \frac{L_k^2}{k^2} \end{aligned}$$

Next, we compute the total cost of calculating all the gradients between checkpoints j and $j + 1$. When the algorithm begins to compute group j , it has j pieces of extra memory, allowing it to further subdivide group j into $j + 1$ intervals. By the intermediate checkpointing lemma, each of these intervals is of length at most $\frac{4(L_{k,j} - 2)}{j - 1} + 1$. We have

$$\begin{aligned} \sum_{i \in \text{group } j} C_{i,k} &\leq j \sum_{l=0}^{\frac{4(L_{k,j} - 2)}{j - 1} + 1} \frac{4(L_{k,j} - 2)}{j - 1} + 1 - l \\ &\lesssim j \left(\frac{4(L_{k,j} - 2)}{j - 1} + 1 \right)^2 \\ &\lesssim \frac{L_{k,j}^2}{j}. \end{aligned}$$

Summing over the at most k checkpoints j , we conclude

$$\begin{aligned} C_k &\lesssim L_k + \sum_{j=1}^k \frac{L_{k,j}^2}{j} \\ &= L_k + L_{k,j}^2 H_k \\ &\lesssim L_k + \frac{L_k^2}{k^2} \log k \end{aligned}$$

where H_k is the k^{th} harmonic number. □

Lemma A.4 (Intermediate Checkpointing). *Consider the behavior of the DTR algorithm using the heuristic h_{e^*} , when computing gradients for the backward pass. Suppose, immediately prior to the computation of gradient \hat{t}_i , we have $2 + k$ pieces of free memory ($k \geq 0$), and that \hat{t}_{i+1} is in memory. Suppose also that forward tensor t_j is the first material ancestor of \hat{t}_i , so that we will rematerialize t_{i-1} starting from t_j to compute \hat{t}_i . Finally, suppose that t_j is never evicted until it is banished.*

Then, immediately after computing \hat{t}_i , memory contains a set of “checkpoint” tensors \mathcal{C} with the following properties:

1. *The tensors in \mathcal{C} remain in memory until they are banished.*
2. *The gap between neighboring tensors in \mathcal{C} satisfies*

$$L \leq \frac{2((i - j) - 1)}{k + 1}$$

Proof. We begin by analyzing the state of memory after computing \hat{t}_i . Since we started with $2 + k$ pieces of free memory, and rematerialized t_{i-1} starting from t_j , Lemma A.3 tells us that, after materializing t_{i-1} , the gaps in memory between t_j and t_{i-1} are all bounded by

$$L \leq \frac{2((i - j) - 1)}{k + 1}.$$

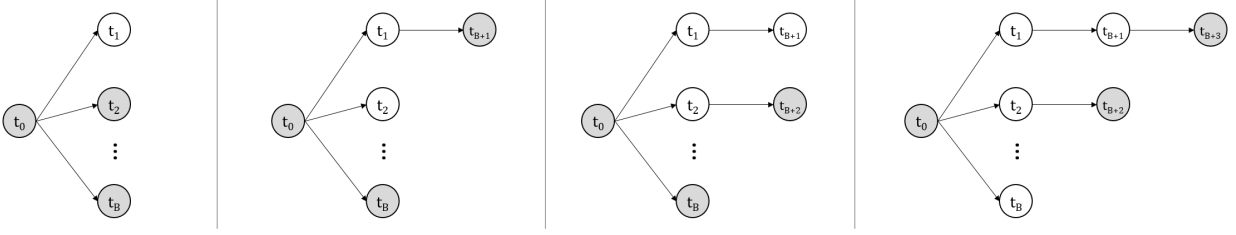


Figure 5: An example construction of an adversarial graph. Gray tensors are in memory (t_0 must always be in memory). The initial tensor t_0 has B paths descending from it, so there is always some path from t_0 with no material tensors. The adversarial construction chooses to place the next node at the end of such an entirely immaterial path.

We need to evict one additional item from memory, in order to compute \hat{t}_i . After this single eviction, the maximum gap is no more than doubled. We conclude that, after computing the first gradient, the maximum gap is no more than $2L$.

It remains to show that the maximum gap in \mathcal{C} does not become larger than $2L$ during the remaining steps of rematerialization. To show this, we first note that the computation of the next gradient, \hat{t}_{i-1} , begins with two units of free memory (having just banished \hat{t}_{i+1} and t_i). We also note that the number of immaterial tensors that need to be rematerialized for this gradient computation does not exceed $2L$. Therefore, when performing the intermediate rematerializations necessary to rematerialize t_{i-2} , it is always possible to evict a tensor with a heuristic value less than $2L$. Since we evict the tensor with the smallest heuristic value, we will never create an immaterial path of length greater than $2L$.

This argument can be applied for every gradient computed between \hat{t}_i and \hat{t}_{j+1} , which shows that the desired properties of \mathcal{C} are maintained. \square

B Proof of Theorem 3.2

In this section, we provide a proof of Theorem 3.2, which lower bounds the number of tensor computations required by DTR under any deterministic heuristic, compared to an optimal checkpointing algorithm.

Proof. We will prove this theorem by designing an adversarially generated graph that forces DTR to repeatedly rematerialize evicted tensors. Our architecture simultaneously leverages the static planner’s ability to reorder computations, to avoid repeated computation of evicted tensors.

Since DTR is a dynamic algorithm, it must choose which tensor to evict at time T based only on the portion of the graph computed up to time T . Our adversarial architecture generator builds the network one node at a time, choosing the next node based on the previous choice of the DTR algorithm. The construction is as follows:

1. The graph begins with tensor t_0 , which, by the behavior of DTR, must remain in memory. Tensor t_0 has B children, t_1 through t_B .
2. After step B of the computation, one of t_0 ’s children must no longer be in memory. Call this evicted child t_* . The next node revealed by the adversary is the child of t_* , causing DTR to rematerialize t_* .
3. The adversary continues to repeat this construction. Since t_0 has B children, but there are only $B - 1$ units of memory to allocate among its descendants, there must be some path from t_0 that contains no material tensors. The adversary reveals the next material tensor on the end of that path, causing DTR to rematerialize the entire path. This repeats until we have revealed all N nodes of the graph.

An example construction of the adversarial architecture is given in Figure 5.

Next, we analyze the computation of DTR on this graph. To do this, we sum the cost of computing each tensor t_1 through t_N . Consider the architecture of the final revealed network, and let L_j denote the length of the path starting from t_j , where $j = \{1, \dots, B\}$ so that t_j is a direct child of t_0 . Since our adversary places the next node such that the

entire path must be rematerialized, the total cost of computing this graph dynamically is

$$\begin{aligned}
 C &= \sum_{j=1}^B \sum_{i=1}^{L_j} i \\
 &= \sum_{j=1}^B \frac{1}{2} L_j (L_j + 1) \\
 &\approx \sum_{j=1}^B L_j^2
 \end{aligned}$$

where \approx hides constant factors. This sum is minimized when the L_j are all equal, which gives $L_j = (N - 1)/B$. The cost of computing all the tensors is therefore at least

$$\begin{aligned}
 C &\gtrsim \sum_{j=1}^B N^2 / B^2 \\
 &= N^2 / B
 \end{aligned}$$

To finish the proof, we upper bound the cost of the optimal static algorithm on this adversarial graph by exhibiting one static checkpointing algorithm and analyzing its behavior. The static algorithm may observe the entire structure of the N nodes, and rearrange the computation in any equivalent order.

Consider the static algorithm that computes the entire graph one path at a time. That is, the algorithm first computes t_1 and all its children (requiring only two units of memory, with no rematerializations), then computes t_2 and all its children (again, reusing the same two units of memory), until all B paths are computed. The total cost is therefore $\Theta(N)$.

We see that DTR requires $\Omega(N^2/B)$ computations to compute the tensors in this graph, whereas a static checkpointing algorithm would only require $\Theta(N)$ computations. We conclude that when DTR is run with a deterministic heuristic, there exists an architecture on which it requires at least $\Omega(N/B)$ times the runtime of a statically checkpointed evaluation. \square

C Simulator Specification

In this section, we provide a detailed technical specification of the DTR simulator. This includes fundamental abstractions, formal definitions of heuristics, pseudocode, runtime optimizations, and details about the log-replaying mechanism.

C.1 Fundamental Abstractions

We based the simulator’s design to support computations logged from PyTorch (see Sec. C.6) and in PyTorch, a tensor is a view (containing metadata) of a buffer; multiple tensors can point to a single buffer. This allows us to model the various aliasing relations between tensors in PyTorch [21]; other DL frameworks likely also make use of similar implementation details.

Storage. At its core, DTR is a runtime system for reducing memory usage. As such, *storages* (i.e., buffers of memory) are the underlying unit which DTR operates on. They support the following operations:

- *size* : **Storage** $\rightarrow \mathbb{N}$: the size of the storage in bytes;
- *root* : **Storage** \rightarrow **Tensor**: the tensor whose parent operation computes the contents of the storage (there is exactly 1 for each storage);
- *tensors* : **Storage** \rightarrow **List**[**Tensor**]: all tensors which view the storage;
- *resident* : **Storage** \rightarrow **bool**: true iff the storage is in memory;
- *locks* : **Storage** $\rightarrow \mathbb{N}$: the number of locks on the storage held internally by DTR (indicating the storage is needed for pending rematerializations);
- *refs* : **Storage** $\rightarrow \mathbb{N}$: the number of external references to the storage, i.e., those held by user code.

We say a storage S is *evictable* if and only if $\text{resident}(S) \wedge \text{locks}(S) = 0$.

Tensor. Each tensor t has an associated “parent” operation $op(t)$ which computes it (potentially along with its underlying storage $storage(t)$).

Each tensor t also has an external reference count $refs(t)$; in particular, each storage S has $refs(S) = \sum_{t \in tensors(S)} refs(t)$. The external reference count is used to track whether a tensor is still live in the source program or whether it should be treated as having been deallocated by the source program. Additionally, t is an *alias* iff $t \neq root(storage(t))$, meaning that t is a view of a storage created by a different parent operator. For convenience, we define $size(t)$ to be 0 if t is an alias and $size(storage(t))$ otherwise (since the metadata will likely be on CPU).

Unlike storages, a tensor t is resident when $storage(t)$ is resident and $op(t)$ has been performed *after* $storage(t)$ last became resident. This condition is denoted as $defined(t)$, and models the behavior of our PyTorch prototype implementation where the whole tensor object is destroyed upon storage eviction (including metadata about the view, like striding and offset)⁸. Thus, before an operation depending on t can be executed, $defined(t)$ must be satisfied, given our assumption that views of a storage must be evicted once the underlying storage has been evicted. Note that for a non-alias tensor t , we have $resident(storage(t))$ if and only if $defined(t)$.

Operator. An *operator* represents a fundamental unit of computation in DTR. Operators are assumed to be pure functions of their arguments, not depending on any other external state (see Sec. C.6 for our handling of mutation). As such, each operator f has an associated compute cost $cost(f) \in \mathbb{N}$. We assume each f has type $\mathbf{List}[\mathbf{Tensor}] \rightarrow \mathbf{List}[\mathbf{Tensor}]$ and define $inputs(f)$ and $outputs(f)$ to be the input and output tensors of f , respectively.

C.2 Formal Metadata Definitions

While our abstract description of DTR in Figure 1 is over tensors, the simulator operates over storages rather than tensors. Thus we must define the metadata our heuristics use over storages, providing notions of cost, staleness, and data dependencies for storages rather than for tensors.

Cost. For a given storage S , we define the compute cost of S as

$$cost(S) := \sum_{t \in tensors(S)} cost(op(t)).$$

This is a worst-case estimation: it represents the compute cost which is incurred when every tensor view of S needs to be rematerialized. An alternative definition is simply $cost(op(root(S)))$, which may be acceptable as aliasing operations are typically much cheaper than non-aliasing.

Staleness. We estimate the staleness of S by tracking the *last access* time of each $t \in tensors(S)$. The last access time $last_access(t)$ is defined as the most recent time when t was referenced by a queued operation. Naturally, we define $last_access(S) = \max_{t \in tensors(S)} last_access(t)$. Staleness, given the current time \mathcal{T} , is then defined as $stale_{\mathcal{T}}(S) := \mathcal{T} - last_access(S)$.

Data dependencies. The dependencies of S are the set of storages

$$deps(S) := \{storage(u) \mid \exists t. t \in tensors(S) \wedge u \in inputs(op(t))\} \setminus \{S\}.$$

Note that we exclude S since it is not a true dependency (each alias tensor in $tensors(S)$ technically “depends” on S). Another possible approximation of the above is to simply take the dependencies of $root(S)$; although this ignores potential dependencies of aliasing operations, it is precise if all aliasing operations only depend on S .

We now define the *dependents* of S as the set $deps^{\top}(S)$ consisting of all T with $S \in deps(T)$. With this definition, DTR can operate over the dependency graph (V, E) where V is the set of storages and $(S, T) \in E$ iff $S \in deps(T)$. Note that (V, E) is implicitly indexed by time \mathcal{T} , with V being the set of non-banished but at-least-once computed storages at \mathcal{T} and E being the dependency relations at \mathcal{T} .

Evicted neighborhood. The *evicted neighborhood* e^* , as defined in Section 3, works without modification over the storage dependency graph. We define it here for completeness. Let $deps_e(S)$ be the evicted subset of $deps(S)$, and likewise for $deps_e^{\top}(S)$. Now, let D_e and D_e^{\top} be the transitive closures of the relations

$$\{(T, S) \mid T \in deps_e(S)\} \quad \text{and} \quad \{(S, T) \mid T \in deps_e^{\top}(S)\},$$

⁸The storage field in a PyTorch tensor is immutable; in principle, we could have changed this to permit reassigning views of evicted storages to point to null and ensure the storages are rematerialized when needed, but this would have required much more extensive modifications to the codebase, which may rely on the invariant of immutable storage pointers.

respectively. Then, $e^*(S) := \{T \mid (T, S) \in D_e\} \cup \{T \mid (S, T) \in D_e^\top\}$. Intuitively, $e^*(S)$ is the set of evicted storages that must be resident to compute all $t \in \text{tensors}(S)$, together with the set of evicted storages T that need S to be resident before all $t \in \text{tensors}(T)$ can be computed.

Relaxed (EqClass) evicted neighborhood. Actually tracking $e^*(S)$ can be computationally expensive due to the directed and changing nature of the graph. For each S , $e^*(S)$ depends on its specific ancestors and descendants; there does not appear to be a simple way of maintaining a single global data structure to track this information as tensors are evicted and rematerialized. A solution will likely involve a dynamic graph connectivity data structure, which would greatly increase the complexity of the simulator’s implementation.

We approach this problem by relaxing the definition of the evicted neighborhood. At a high level, our solution works as follows: given a storage dependency graph $G = (V, E)$, we first forget edge directions to obtain the undirected dependency graph \tilde{G} . Now, let \tilde{G}_e be the subgraph obtained by removing all resident storages (and any edges including them). Each connected component of \tilde{G}_e is then an *evicted component*, with each evicted $T \in V$ belonging to exactly one component $\epsilon^*(T)$. Then, the (relaxed) evicted neighborhood for a resident storage S is defined as

$$\tilde{e}^*(S) := \left(\bigcup_{T \in \text{deps}_e(S)} \epsilon^*(T) \right) \cup \left(\bigcup_{T \in \text{deps}_e^\top(S)} \epsilon^*(T) \right).$$

Note the structural similarity in this definition with $e^*(T)$; they are indeed similar, but $\tilde{e}^*(S)$ overapproximates the neighborhood by ignoring edge directions. Each evicted component can be efficiently represented using a *Union-Find* (or *disjoint-set*) data structure with very good asymptotic complexity for merging and obtaining static set metadata. In the case of DTR, each component tracks the sum of the compute costs of its elements (with the union of two components having the sum of each constituent cost). This enables very cheap querying of compute costs over $\tilde{e}^*(S)$.

However, despite this optimization, *splitting* is not a supported operation on disjoint-sets.⁹ Approaches to splitting would also need to recover the original compute costs of each set, which may require traversing the whole set if done naively. Unfortunately, DTR regularly splits evicted components during rematerialization. In order to deal with this, we use the following overapproximation: when a (previously) evicted storage S belonging to $\epsilon^*(S)$ is rematerialized, we set $\epsilon^*(S).cost := \epsilon^*(S).cost - cost(S)$. While resident storages thus never count towards the compute cost of a component, “phantom connections” between evicted storages may accumulate over time (likely depending on the connectedness of the underlying dependency graph). Despite this limitation, this approximation worked well in practice, as can be seen in the simulated and prototype results.

C.3 Formal Heuristic Definitions

Having defined the metadata above, we can now formally define the h_{DTR} variants used in Sec. 4.1. (Recall that h_{DTR} heuristics compute a score using measures of size, computational cost, and staleness and evict the tensor with the smallest score, corresponding to the intuition that the tensor evicted should be large, unlikely to be rematerialized, and cheap to rematerialize if it does need to be rematerialized.)

$$\text{DTR-Full}(S) := \frac{cost(S) + \sum_{T \in \epsilon^*(S)} cost(T)}{size(S) \cdot stale_{\mathcal{T}}(S)}.$$

$$\text{DTR-EqClass}(S) := \frac{cost(S) + \sum_{T \in \tilde{e}^*(S)} cost(T)}{size(S) \cdot stale_{\mathcal{T}}(S)} \approx \frac{cost(S) + cost^*(S)}{size(S) \cdot stale_{\mathcal{T}}(S)}$$

Note that the simulator implementation uses the splitting approximation described above, with $\tilde{e}^*(S)$ depending on the specific sequence of evictions and rematerializations. $cost^*(S)$ in the second expression is used to denote this statefulness.

$$\text{DTR-Local}(S) := \frac{cost(S)}{size(S) \cdot stale_{\mathcal{T}}(S)}.$$

⁹This can be seen as a variant of the Union-Find-Split problem, which typically requires the use of more complex data structures such as link-cut trees.

C.4 Implementation Details

Runtime state. In what follows, we denote the collective runtime state of the DTR simulator as R , and use the dot notation to indicate stateful reads and writes of runtime values. The simulator tracks the following runtime state:

- $R.\text{heuristic} : (\text{Storage}, \text{Metadata}) \rightarrow \mathbb{R}$, the eviction heuristic, interpreted as a score (the lowest-scored storage is evicted);
- $R.\text{budget} : \mathbb{N}$, the memory budget in bytes;
- $R.\text{memory} : \mathbb{N}$, the current memory usage in bytes;
- $R.\mathcal{T} : \mathbb{N}$, the current clock time in some unit of granularity, such as nanoseconds;
- $R.\text{pool} : \text{List}[\text{Storage}]$, list of all currently evictable storages.

Eviction and banishing. To evict a given storage S , we set all tensors in S to be undefined, remove S from the pool, and decrease $R.\text{memory}$ by $\text{size}(S)$. Cached metadata are also updated as necessary.

Banishing (*permanent* eviction) is slightly more subtle; in particular, it can only be done for S when $\text{deps}_e^\top(S) = \emptyset$. Banishing then proceeds by evicting S as above, but with the additional effect of removing S entirely from the dependency graph. Each $T \in \text{deps}^\top(S)$ is then locked (and effectively becomes a non-rematerializable constant). Storages locked in this way are said to be *pinned* (and have a special flag in the simulator), to distinguish them from those locked during rematerialization, and we permit them to be banished in the future. Note that banishing can be performed on evicted S when the above condition is met, in which case the eviction is skipped.

(Re)materialization. When a tensor t is to be (re)materialized, its parents’ storages are first locked by incrementing the lock count (so that they don’t get evicted while they are still needed) and undefined parents are recursively rematerialized. We then increment $R.\text{memory}$ by $\sum_{u \in \text{outputs}(op(t))} \text{size}(u)$ (performing evictions as necessary), and move $R.\mathcal{T}$ forward by $\text{cost}(op(t))$. Multi-output operations must be handled carefully so as to not leak memory: we make sure to *decrease* $R.\text{memory}$ by $\text{size}(u')$ for each $u' \in \text{outputs}(op(t))$ that was defined *prior* to the rematerialization. This models the immediate freeing of doubly-computed ephemeral tensors in the PyTorch implementation. Lastly, locks on parent storages are freed and unlocked storages (including any newly rematerialized ones) are added back into $R.\text{pool}$.

Constants. The simulator models non-rematerializable constants like weights and inputs by creating dummy “constant” tensors using nullary operators with 0 cost and pinning the resulting storage. This allows the simulator to have a full picture of the computation graph. Furthermore, log-accurate banishing requires knowledge of constants (as PyTorch reference-counts constants).

C.5 Additional Runtime Optimizations

Banishing and eager eviction. When the final external reference to a storage S is lost, we know that the underlying DL framework would have reclaimed the memory used by S . To utilize this information as opposed to doing nothing, we can either banish S or simply evict S normally. When banishing, must first check that S has no evicted dependents; if it does, then we retry banishing each time a dependent is rematerialized. Banishing has the ability to evict constants, but at the downside of pinning potentially exploding amounts of memory. The alternative (*eager eviction*) is easier to implement and simply involves evicting S normally (if possible). This prevents the problem of over-pinning memory, but with the downside that constants can never be evicted. In practice, eager evictions allowed us to save more memory (see Sec. D.2 for details).

Caching metadata. To avoid costly recomputations of metadata during heuristic evaluations, we cache the local cost $\text{cost}(S)$ for each S (as it only changes when new aliases are made). Additionally, for the DTR-Full heuristic, we avoid recomputing $e^*(S)$ at each evaluation by caching and only recomputing after evictions or rematerializations that directly affect $e^*(S)$. Such recomputations are further optimized by tracking the evicted ancestors and descendants separately (allowing them to be recomputed independently, depending on the position of the affected storage).

C.6 Log-Replaying Mechanism

Log format. We logged PyTorch operations as a sequence of abstract instructions corresponding to the semantics of the actions we were easily able to instrument in the framework. Every PyTorch tensor is given a unique identifier string upon creation, which is recorded and used in the log. In this section, each PyTorch tensor t corresponds to a simulator tensor $\llbracket t \rrbracket$.

The log contains the following instructions:

- **MEMORY**($t, size$): logs that t uses $size$ memory; treated as 0 if $\llbracket t \rrbracket$ is an alias.
- **ALIAS**(t_o, t_i): logs that $\llbracket t_o \rrbracket$ is an alias of $\llbracket t_i \rrbracket$, i.e., two different views of the same storage. t_i can either be a tensor identifier or \perp ; if $t_i = \perp$, then t_o does not alias another tensor (t_o 's parent operation created its storage).
- **CALL**($inputs, outputs, cost, op$): logs the operator call $outputs = op(inputs)$ with compute cost $cost$. This instruction is followed by $|outputs|$ **MEMORY** and **ALIAS** instructions to log information about each output. Each **CALL** corresponds to a simulator operator $\llbracket op \rrbracket$ with inputs $\{\llbracket i \rrbracket \mid i \in inputs\}$ and new simulator tensor outputs $\{\llbracket o \rrbracket \mid o \in outputs\}$.
- **MUTATE**($inputs, inputs', cost, op$): logs the in-place (mutating) operator call $op(inputs)$ with compute cost $cost$, which modifies $inputs' \subseteq inputs$.
- **CONSTANT**(t): logs that $\llbracket t \rrbracket$ is a constant, and is followed by a **MEMORY** instruction.
- **COPY**(t_o, t_i): logs a new identifier t_o with $\llbracket t_o \rrbracket = \llbracket t_i \rrbracket$. This increments $refs(\llbracket t_i \rrbracket)$. This happens when Python code like “ $x = y$ ” is called where y is a PyTorch tensor and x is a fresh variable; this action neither creates a new storage nor a new view but only has x point to the same view as y .
- **COPYFROM**(t_o, t_i): logs the PyTorch code $t_o = t_i$ where each side is an existing tensor. This decrements $refs(\llbracket t_o \rrbracket)$, increments $refs(\llbracket t_i \rrbracket)$, and updates $\llbracket t_o \rrbracket \mapsto \llbracket t_i \rrbracket$. Intuitively, this corresponds to Python code like “ $x = y$ ” where y is a PyTorch tensor and x was already assigned to a PyTorch tensor; in PyTorch, x is mutated to match y .
- **RELEASE**(t): logs the destructor of the PyTorch tensor t . This decrements $refs(\llbracket t \rrbracket)$.

Supporting mutation. To support mutation from in-place operators, the simulator adds a “reference layer” that mutates cloned tensors, allowing for a uniform interface for all operators. Given a mutation instruction **MUTATE**($inputs, inputs', cost, op$), let i_{new} be a new unique identifier for each $i \in inputs'$, and let $inputs'_{new} = \{i_{new} \mid i \in inputs'\}$. We then proceed by treating op as a pure operator from $inputs$ to $inputs'_{new}$, where each newly created simulated tensor $\llbracket i_{new} \rrbracket$ is non-aliasing and has size $size(storage(\llbracket i \rrbracket))$. Lastly, we decrement $refs(\llbracket i \rrbracket)$ and update the mapping $\llbracket i \rrbracket \mapsto \llbracket i_{new} \rrbracket$. Intuitively, we are modeling the transformation

$$op(t) \rightsquigarrow \text{Tensor } t' = copy(t); op(t'); t = t'.$$

Note that in our prototype implementation, a mutation of i may produce incorrect results when $\llbracket i \rrbracket$ is an alias, since the mutation layer would create a clone but aliases would still point to the old storage. Potential solutions in real implementations would be to propagate the above rewrite to all aliases of a storage (costly) or to mutate storage pointers (which would have increased the complexity of our modifications to PyTorch).

Output condition. All live tensors at the end of a log (i.e. all t with $refs(t) > 0$) are treated as outputs which the users want (i.e. gradients, loss, prediction). They are thus rematerialized (if evicted) and locked to ensure they persist. This prevents the simulator from incorrectly reporting better results by evicting computed weight gradients and never rematerializing them. This permits the user to perform the weight update step outside of DTR immediately after the backward pass ends. Based on our observations of PyTorch’s optimizer gradient updates, we could also support performing these updates within DTR, since a parameter update simply performs in-place mutating additions (`add_`) of scaled gradients to the parameters.

D Ablation Study

In this section, we present an ablation study comparing the impacts of different sources of information for the h_{DTR} heuristic, as well as comparing the eager eviction deallocation policy used in the h_{DTR} heuristics with the alternative of banishing. In addition to comparing the overhead in terms of additional tensor computations, we also compare the runtime overhead of different h_{DTR} configurations in terms of the number of tensor accesses by heuristic computations and metadata updates. These trials were performed using the same logs as in Sec. 4.1.

D.1 Data Sources

First, we will analyze the three sources of information (metadata) for the h_{DTR} heuristic. Recall that $h_{DTR}(s, m, c)(t) = c(t) / [m(t) \cdot s(t)]$, where s is a measure of staleness, m is a measure of size, and c is a measure of compute cost. For this study, we take s and m to be the staleness and size functions defined in Appendix C. For

compute cost c , we compare the following alternatives (see Appendix C for definitions): the full e^* , the approximation \tilde{e}^* , and the local cost (cost of the parent operator only). We allow each measure to be entirely ablated (e.g., $s(t) = 1$, which we denote $s = \text{no}$).

In the following figures, we specifically have $s, m \in \{\text{yes}, \text{no}\}$ and $c \in \{e^*, \text{EqClass}, \text{local}, \text{no}\}$. Each figure fixes a choice of c , varying s and m .

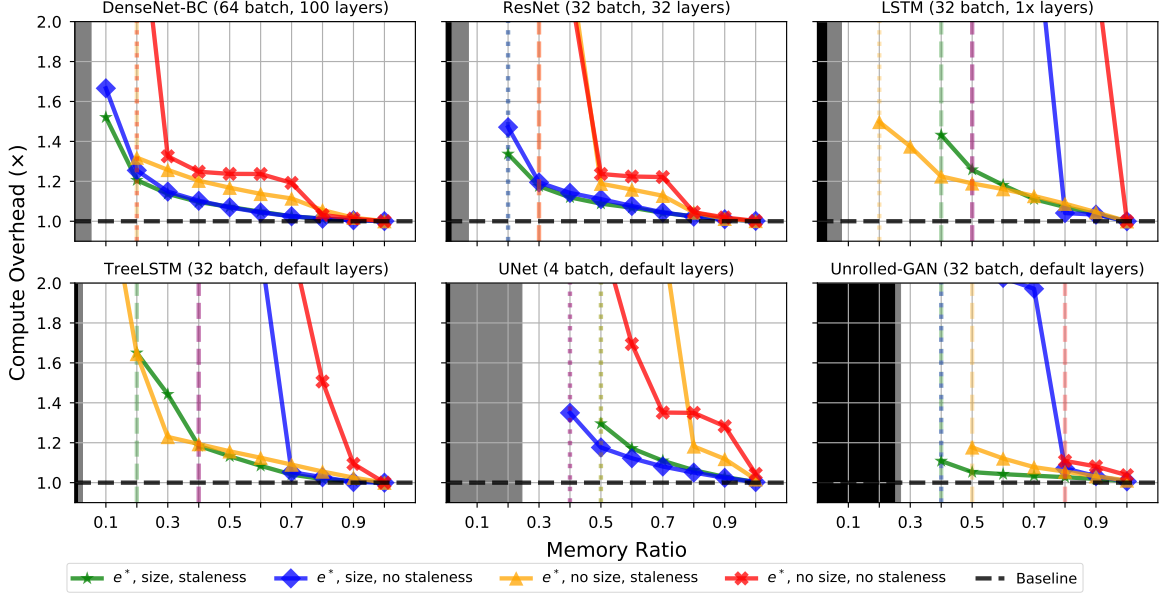


Figure 6: Results for fixed $c = e^*$, varying s and m .

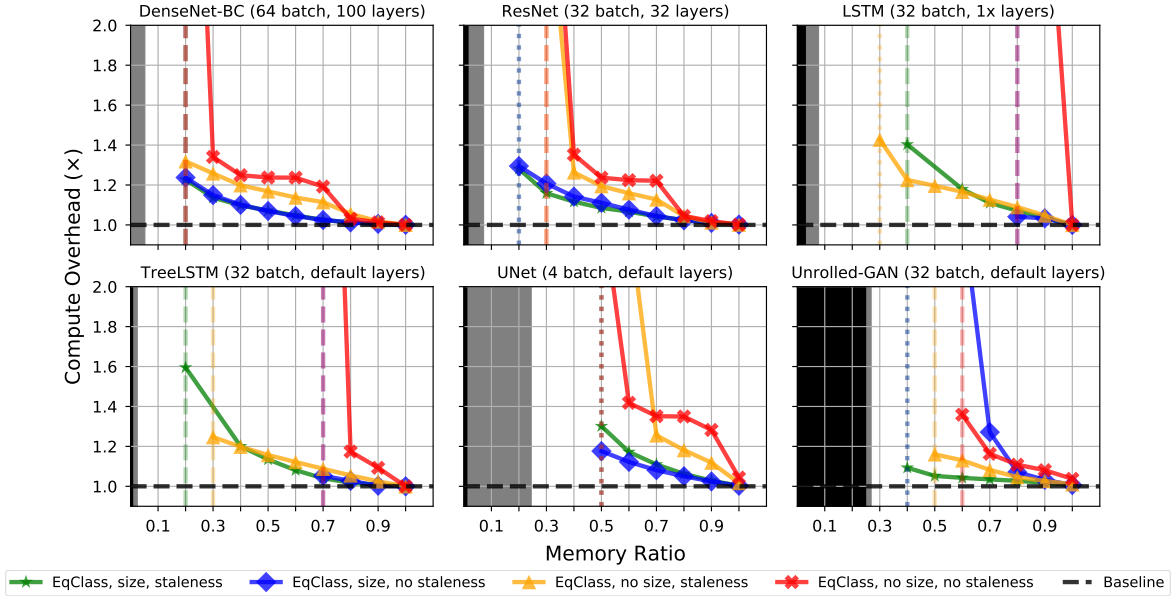
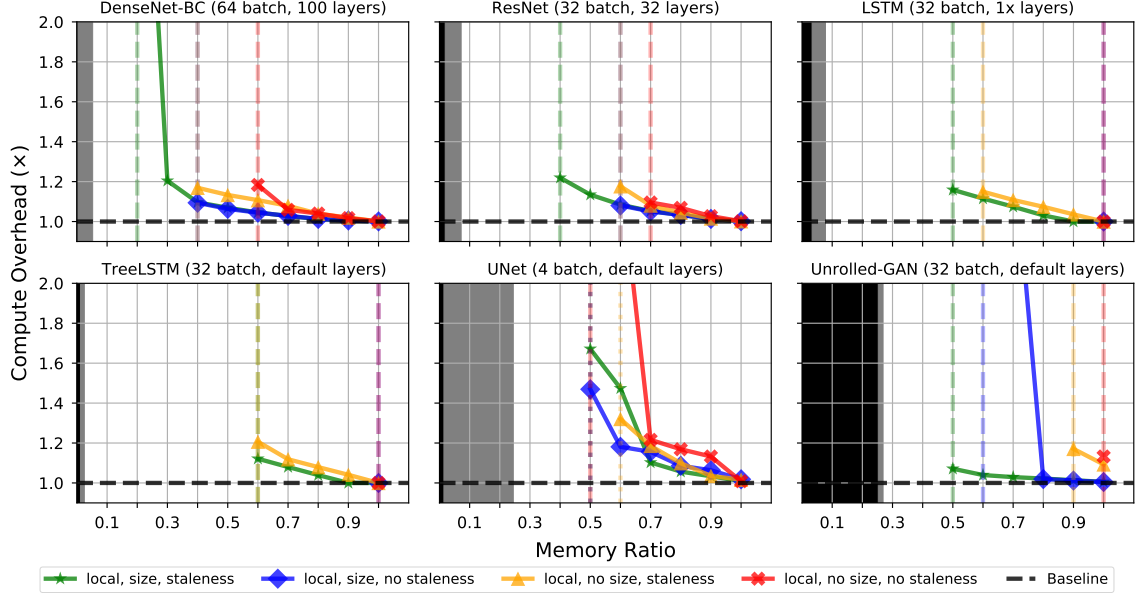
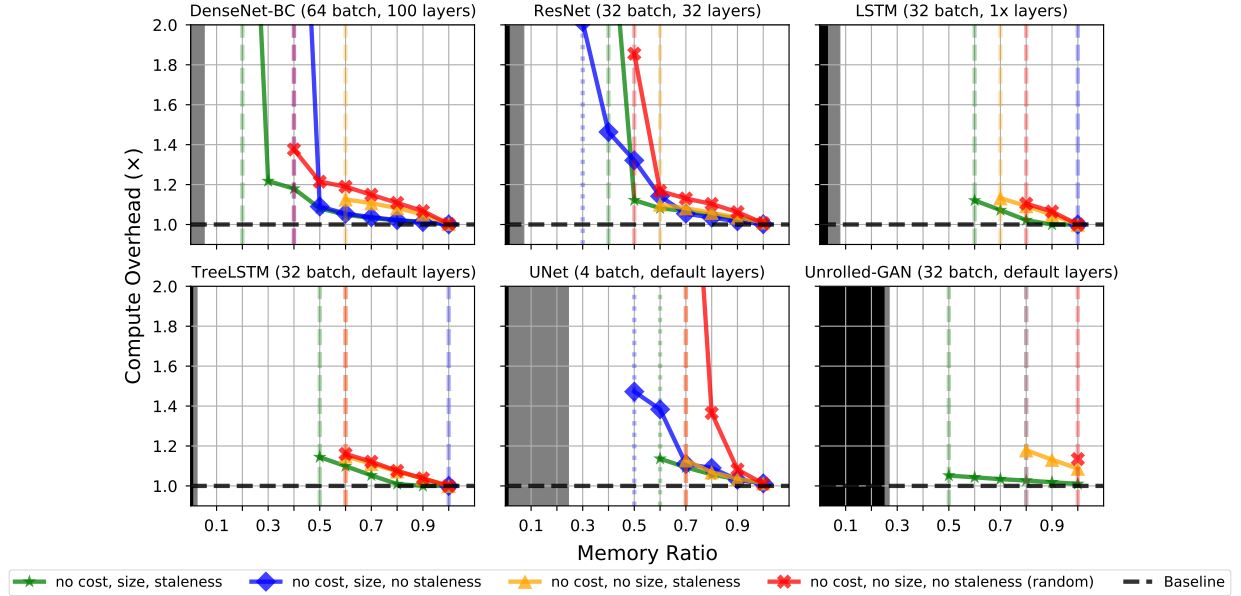


Figure 7: Results for fixed $c = \text{EqClass}$, varying s and m .

The general trend shown in Figures 6, 7, 8, 9 is that higher metadata complexity (corresponding to more precise notions of the evicted neighborhood) enables more savings, while staleness and size are required for acceptable computational overhead. It is interesting to note that the importance of staleness and size is dependent on the specific model architecture. For example, cost and size alone does far better than cost and staleness for the static models (DenseNet, ResNet, UNet),

Figure 8: Results for fixed $c = \text{local}$, varying s and m .Figure 9: Results for fixed $c = \text{no}$, varying s and m .

whereas the opposite is true for the dynamic models. This may be due to model depth or the distribution of tensor sizes or to the increasing impact of individual checkpoints at lower budgets; further research may shed more light on the influence of model-specific characteristics like these. Additionally, we may note that the \tilde{e}^* approximate cost performs comparably to the e^* exact cost requiring less information, validating our belief that the equivalence classes are a useful approximation.

In general, the best-performing of these h_{DTR} heuristics were those with non-ablated choices of s , m , and c , hence our choosing the h_{DTR} variants with e^* , \tilde{e}^* , and local cost (DTR-Full, DTR-EqClass, and DTR-Local, respectively) for the evaluation in Sec. 4.1.

D.2 Banishing

For the following trial, we compared the DTR-Full heuristic with banishing (permanent removal) against that with eager evictions, as described in Appendix C.5. We only used e^* cost because it performed much better than local cost and because it would have been more complicated to update the definition of \tilde{e}^* to account for banished neighbors.

The results are shown in Figure 10.

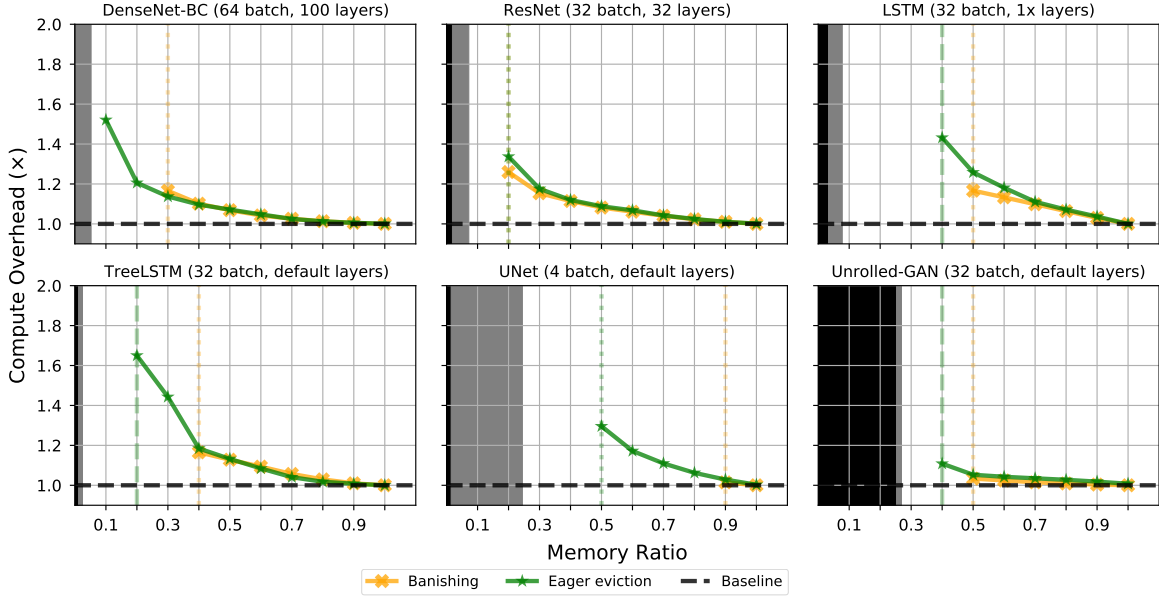


Figure 10: Results for the DTR-Full heuristic, comparing banishing and eager evictions.

As the curves show, banishing is not able to achieve the same level of savings across most models tested as eager eviction. For UNet, the difference is large: banishing can only save 10% memory (and OOMs at 0.8 ratio), while eager eviction allows for 50% savings. However, banishing still achieves good savings on most models, even obtaining better computational overhead under the same budget and savings for ResNet. Since banishing potentially allows for greatly lowered runtime overhead, implementations of DTR can consider conditionally enabling it in situations where the tradeoff is more desirable.

D.3 Runtime Overhead

For this experiment, we tracked the number of storage (see Appendix C.1) accesses made during evaluations of heuristics and maintenance of metadata. We chose this metric over wall-clock time, since our Python implementation of the simulator is not heavily optimized and could potentially fail to reflect the real performance of the algorithm. Storage accesses, on the other hand, do reflect operations that would be performed by a real implementation. For the DTR-Full heuristic, this included each storage visited during the updating and rebuilding procedures for maintaining e^* for resident storages. For the DTR-EqClass heuristic, this included each storage visited whenever the Union-Find data structure was traversed for each evicted component (which occurs mainly during merging and when reading the compute cost). The DTR-Local heuristic does not need to maintain any non-local metadata. For all heuristics, each heuristic evaluation counted as one storage access.

As Figure 11 shows, the accesses made by each heuristic are generally separated by at least an order of magnitude. This confirms our intuitions about the runtime overhead of each heuristic, and supports our choice of DTR-EqClass as a good middle ground (in terms of both runtime and computational overhead). However, these overhead figures could be improved with better-optimized implementations of the heuristics, as our implementation recomputes heuristics often, even when it may be possible to store the scores for tensors and maintain them in a sorted order. (Reformulating staleness to avoid having to use the current time might help.) Using persistent data structures that can be incrementally updated and maintain a sorted order will make these heuristics much more efficient, though this would also increase the complexity of the implementation.

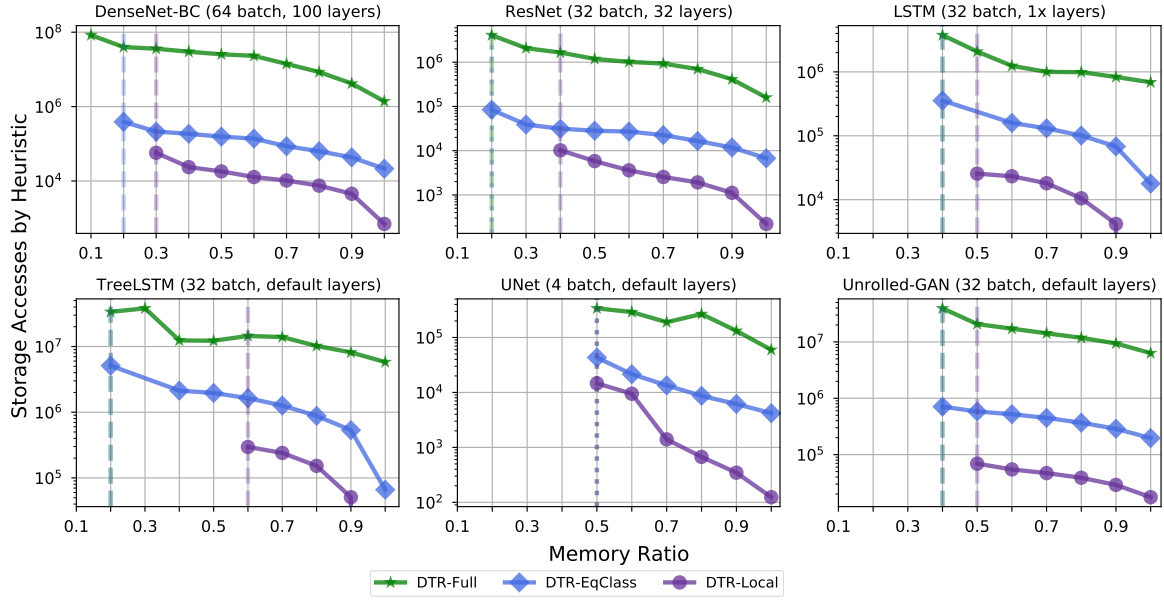


Figure 11: Total storages accesses incurred by heuristic evaluations and metadata maintenance, compared across different memory ratios, for the 3 main h_{DTR} variants.